CHAPTER VI

Modes of Motion in Quartz Crystals, the Effects of Coupling and Methods of Design

By R. A. SYKES

6.1 Introduction

WITH the recent extended use of Quartz crystals in oscillators and electrical networks has come a need for a comprehensive view of the various types of crystal cuts. In addition there has been a need for illustration of some of the methods employed in choosing the proper cut for a given requirement, the manner in which quartz crystals vibrate and the basic principles governing the choice of a design to use certain cuts most advantageously. In particular one of the greatest problems associated with the recent large scale production of crystals for oscillator purposes has been that of obtaining crystals the activity and frequency of which would not vary to any large degree over a wide range in temperature.

It is the intention of this chapter to present a physical picture of the manner in which quartz crystals vibrate in their simplest forms and then to show what has been learned from these simple forms that will apply to the more complex combinations of motion. The motion of a bar or plate is determined almost wholly by its dimensions and the particular type of wave generated, or frequency applied, and very little upon the driving system if the coupling to the driving system is small. In the case of quartz the coupling between the electric and mechanical system is small and hence we may study the motion of rods and plates without always considering the effect of changes due to the method of excitation (i.e., piezo-electric). However the ease of exciting and measuring a particular mode does depend on the piezo-electric constant driving it. Basically only three types of motion will be considered; flexural, extensional and shear. These three types of motion or combinations of these can be considered to represent most of the cases with which we will concern ourselves. In addition, the frequency equations will be given for common types of motion and the effect of coupling between various modes of motion. Finally the general rules relating to the dimensioning of oscillator plates will be presented.

6.2 Types of Motion in Quartz Rods and Plates

6.21 *Flexural*

The motion associated with flexure will be discussed first because this is the type of motion that we see more commonly in nature. This motion is

the type which presents itself in the xylophone, the chime type door bell, and various other vibrating reeds or bars. Fig. 6.1 shows the general type of motion of a bar free to vibrate in flexure. The displacement takes place in the direction of W and the wave is propagated along the length. A flexure mode is one in which the center line does not change length. The type of motion associated with the first order, or fundamental, of a bar free to vibrate on both ends is shown in Fig. 6.1 with a dotted figure superim-

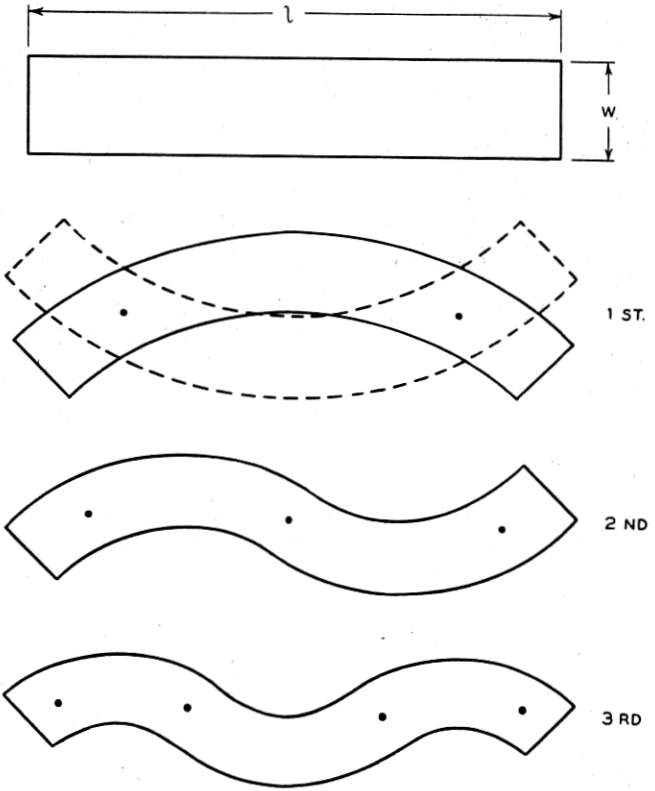

Fig. 6.1—Motion of a bar in free-free flexure.

posed to show the motion in the opposite phase. The straight bar then would be distorted first in one direction and then in the direction of the dotted figure. In the case of the second mode of vibration, it will be noticed that it consists essentially of two of the fundamental mode types joined end to end. This is not strictly the case, but serves to illustrate the motion. The dots shown at various points on the bar show positions of zero motion or nodes. In the case of the fundamental mode, there are two nodes and in the second and third there are three and four respectively. One point of

interest in flexure vibration as seen in Fig. 6.1 is that the ends of the bar will be vibrating in the same direction for odd order modes and the motion of the two ends will be in opposing directions for even order modes. The frequency of a bar vibrating in flexure may be easily computed for low orders when the width is small in comparison with the length. When the width is appreciable other factors must be considered as will be shown later. In general, the flexure frequency of a bar will be the lowest frequency of vibration.

In the case of a plate where we are concerned with flexural vibrations propagated along the length with motion in the direction of the thickness it

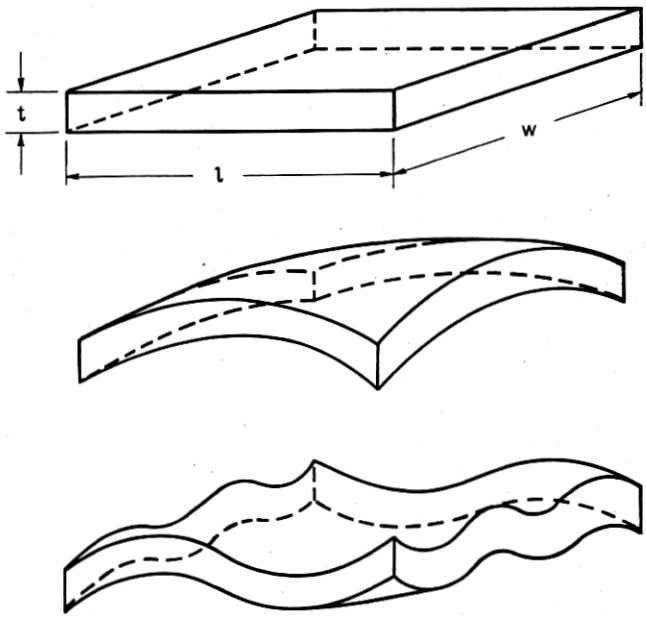

Fig. 6.2—Motion of a plate in free-free flexure.

is necessary to consider also the width. As noted in Fig. 6.1, our concern was only for a bar of small third dimension. When considering the case of a plate in flexure along its length and thickness, then the third dimension must also be considered for more complicated types of motion. In a manner somewhat similar to the vibration of a bar, we can consider a plate vibrating in its thickness-length plane. Since a plate also has width, we must also consider this dimension. The simplest type of motion would be that of a simple flexure which would bend the plate into the shape of an arch. If now, the third dimension is permitted to flex, the distortion of a plate shown in Fig. 6.2 could be illustrated by a flexure in the ℓ–t plane and in the

w–t plane. Considering the motion of the plate as a flexure vibration along the length vibrating in the thickness, then we may also have a distortion along the width and thickness corresponding to similar or higher types of flexure motion. The illustration at the bottom of the figure shows a plate vibrating in its second order flexure along the length and thickness and the fourth order flexure along the width and thickness. The effect of these higher orders in the w–t plane is to slightly modify the frequency of the ℓ–w mode.

A thorough treatment of this type of double flexure in plates will be given in Chapter VIII by H. J. McSkimin.

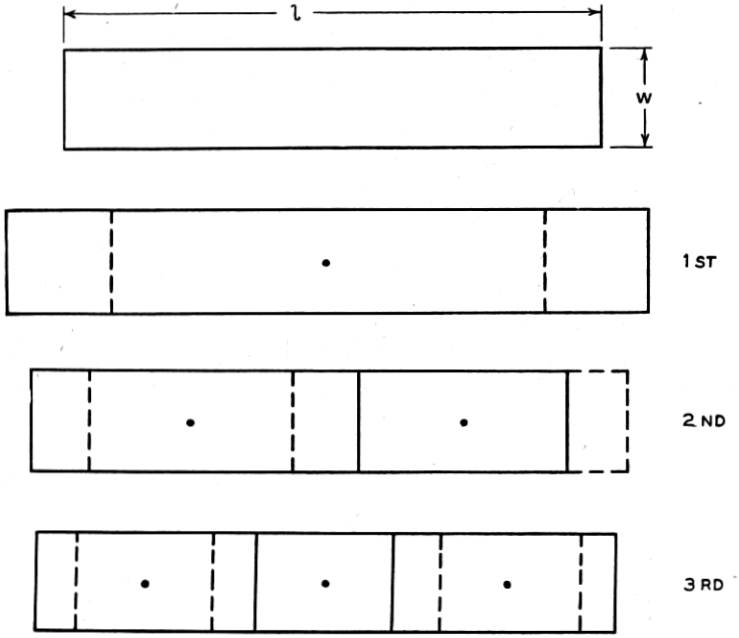

Fig. 6.3—Motion of a bar in free-free extension.

6.22 *Extensional*

The extensional or sometimes termed longitudinal motion of a bar free to vibrate is shown on Fig. 6.3. This motion is somewhat simpler than the flexure motion and consists simply of a displacement in the direction of the length of the bar of a wave propagated along the length. This means that the first mode of vibration will be simply an expansion and contraction of all points with respect to the center of the bar. This motion will be along the length. The displacements along the bar will then be in proportion to the sine of the angular distance from the center. The distortion of a free bar in its simplest mode is then illustrated in Fig. 6.3 labeled 1st. Since the

motion must be dynamically balanced, a node will appear at the center of the bar, and the bar will grow longer and shorter as shown by the solid and dotted lines. In the case of the second order of motion, as shown in Fig. 6.3, it consists essentially of two 1st order modes joined together at their ends and of opposite phase. That is to say, when one half of the bar is expanding, the other half is contracting. In the case of the 3rd mode, as can be seen from Fig. 6.3, the central element is contracting while the external elements are expanding. From this we may state generally, that for odd order types of motion, the extreme ends of the bar will be expanding or contracting in phase and for even order modes, the extreme ends will be expanding or contracting in opposite phase. Fig. 6.3 illustrates extensional motion in its simplest form. In a practical case an extension in one direction is accompanied by a contraction in one or both of the other two dimensions. This of course is due to elastic coupling and will be considered more in detail later. If we consider a rectangular plate it is not difficult to imagine that it would have three series of extensional modes of vibration due to the three principal dimensions.

6.23 *Shear*

The low frequency of face shear type of motion of a plate is somewhat more complicated than either the flexure or longitudinal and, as shown in Fig. 6.4, consists simply of an expansion and compression in opposite phase along the two diagonals of the plate. This motion is shown in Fig. 6.4 labeled $m = 1, n = 1$. The two phases are shown, one a solid curve and the other a dotted curve to illustrate the distortion with respect to the original plate. One peculiarity of shear motion in plates is that it may break up into motions similar to its fundamental along either the length or the width. For example, if we take the motion associated with $m = 1$, $n = 1$, and superimpose two of these in opposite phase on the same plate, we would get the type of motion illustrated by $m = 2, n = 1$. In a similar manner, the motion may reverse its phase any number of times along either the length or the width. One particular case is shown for $m = 6, n = 3$. As can be seen from the case of $m = 1, n = 1$, the distortion is not that of a parallelogram as it is in the static case because here we are concerned only with the dynamic case. While the equation of motion of a free plate vibrating in shear has not been completely solved, a microscopic analysis indicates that the actual motion of the plate edges appear to be somewhat as shown for the case $m = 1, n = 1$ when driven in this mode.

The shear mode of motion in the case of a thin plate is somewhat different for the high frequency case than for the low frequency case. In the case of high frequency shear modes of motion in thin plates, the motion of a particle is at right angles to the direction of propagation which in this case would be

the thickness. The simplest type of motion for high frequency shear is shown in Fig. 6.5 where the top of the plate is displaced in the direction along ℓ with respect to the bottom of the plate. This would then be termed the length-thickness shear. When viewed from the edge of the plate, the motion is very similar to that shown in Fig. 6.4 for the case of $m = 1, n = 1$. In a manner similar to the previous case of shear the front edge of the plate may be divided into segments along ℓ and along t. For example, we may get

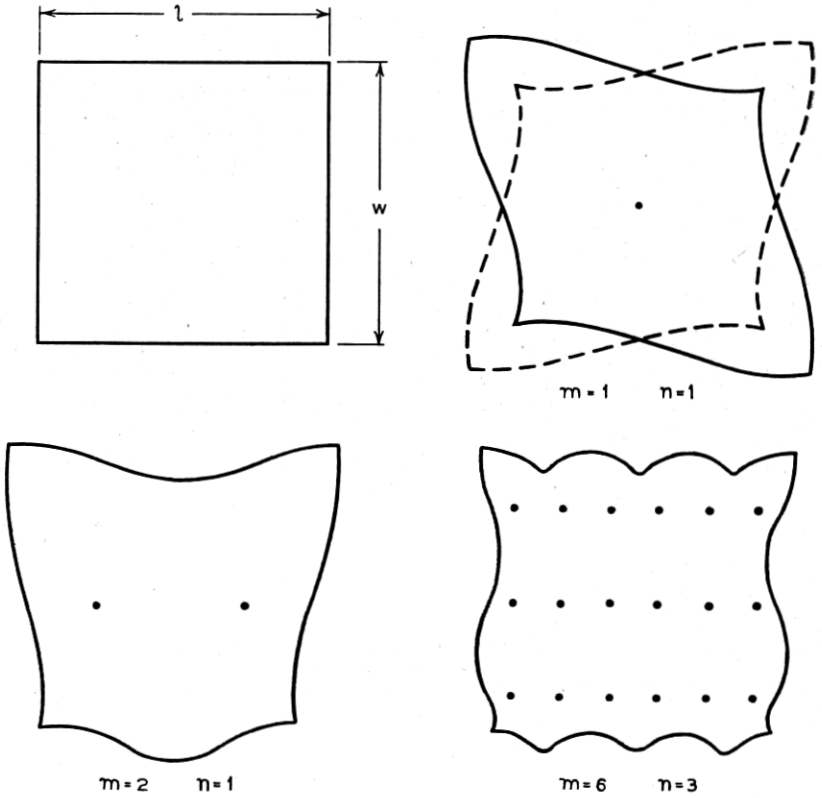

Fig. 6.4—Motion of a plate in low frequency shear.

a double shear along ℓ with a single shear along t. This case is illustrated in Fig. 6.5 for $m = 1, n = 2$ and $p = 1$. In general, m and n may assume any integral value. As in the case of flexure we must also consider the third dimension. The motion associated with the third dimension may be represented by simple reversals of phase as before. For example, in Fig. 6.5 the case for $m = 1, n = 1, p = 2$ is shown which simply means that the high frequency shear on the front half of the plate is out of phase with that of the

back half of the plate. This discussion relates only to the case of the high frequency shear commonly assumed to be a single shear along the length and thickness of the plate. Similar statements can be made if we consider the high frequency shear as being along the width and thickness.

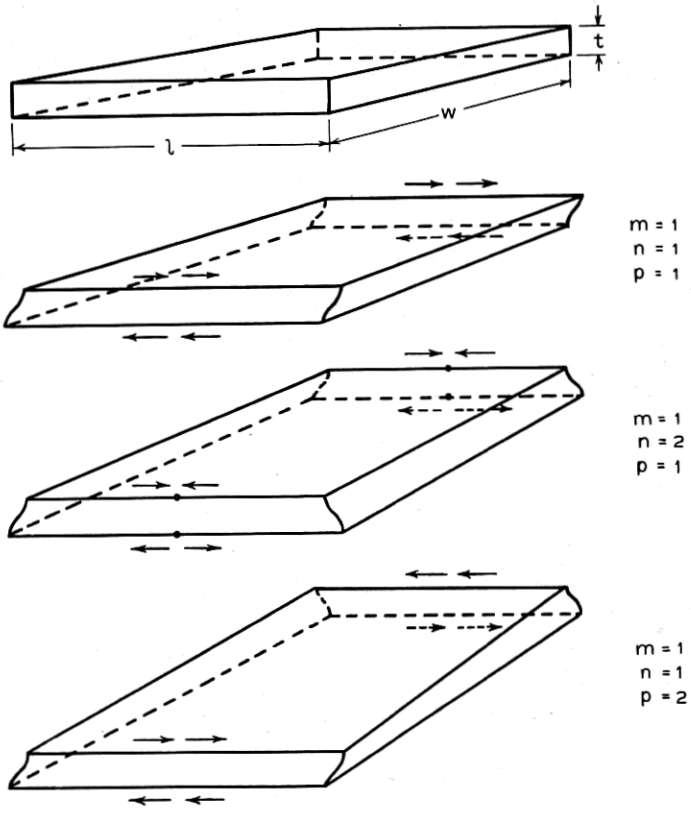

Fig. 6.5—Motion of a plate in high frequency shear.

6.24 *Type of Motion for Some Standard Filter and Oscillator Plates*

To get a more complete picture of the applications of the various types of motion, we will now take specific cases. The various crystals as commonly used for oscillators or filters are shown in Fig. 6.6. At the top of Fig. 6.6 are shown the various types of shear plates with their relative position with respect to the crystallographic axis.

The *AT* and *BT* plates are termed high frequency shear plates and the motion associated with them is that of a length-thickness shear as shown in Fig. 6.5. Their use is found for the control of radio frequency oscillators in

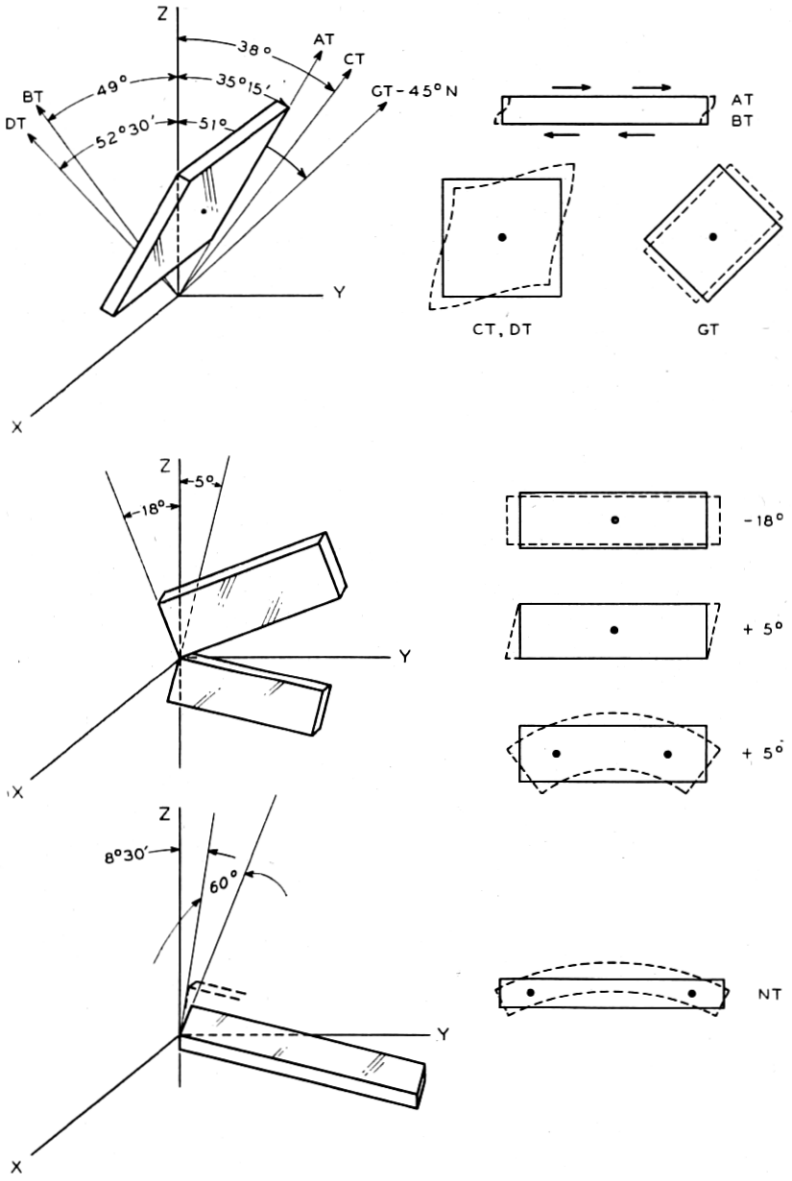

Fig. 6.6—Motions of typical cuts of quartz.

the range from 1 to 10 megacycles. The *AT* is most useful in the lower range and the *BT* in the upper range since it has a higher frequency constant.

Considerable use for the AT plate has been found for filters on pilot channels for the coaxial telephone system.

The CT and DT are analogous to the AT and BT but are termed low frequency shear plates. The motion associated with these cuts is that of a face shear as illustrated in Fig. 6.4. The CT and DT cuts are useful for both filter and oscillator applications in the frequency range from 60 kilocycles to 1000 kilocycles. Here again the DT would be most useful in the lower range and the CT the upper range due to the higher frequency constant for the CT cut.

The GT is similar to the CT except that it is rotated by 45° about the normal to the plate so that instead of a face shear type of motion there are two extensional modes similar to that shown in Fig. 6.3. These two modes are coupled to each other resulting in one of them having a zero temperature coefficient over a wide range of temperature. This crystal is most useful in the range from 100 kilocycles to 500 kilocycles for a primary standard of frequency and in filter networks having extreme phase requirements.

The filter plates commonly called the $-18°$ cut and 5° cut are shown with their relation to the crystallographic axes in the central part of Fig. 6.6. The $-18°$ cut commonly used in filters employs a simple extensional motion along its length with small coupling to an extensional motion along its width and practically zero coupling to a face shear type of motion. Since the width is usually the order of half the length these modes are not troublesome. The $+5°$ cut is useful in filter work because it has a low temperature coefficient and in spite of its strong coupling to the plate shear, it has been found quite useful in both its extensional mode and its flexure mode. The $-18°$ cut is used over the frequency range from 60 kilocycles to 300 kilocycles and forms the basic crystal used in the channel filters of the coaxial telephone system. When driven in flexure the 5° cut may be made to operate as low as 5 kilocycles and is used in oscillator and filter circuits.

The NT cut is shown at the bottom of Fig. 6.6 with its relation to the crystallographic axis. This is obtained by a rotation of $+8.5°$ about the X axis with a second rotation of $\pm$ 60° about the resulting Y' axis. The purpose of the second rotation is to give the shear modulus a positive coefficient. This modulus enters into the equation for the flexure frequency and therefore the effect of the second rotation is to change the temperature coefficient of the flexure mode from a negative value to zero. This crystal has been used to some extent as a low frequency oscillator. Its main purpose so far has been for the control of frequency modulation broadcast transmitters and for low frequency pilot channel filters.

Another crystal called the MT which is cut in a manner similar to the NT but with angles of 8.5° and 36° respectively has been used for filter work where an extensionally vibrating crystal of zero temperature coefficient is

required. The motion associated with this crystal is similar to that shown for the $+5°$ cut of Fig. 6.6. The low temperature coefficient is obtained through coupling to, and the effects of, a shear mode of positive temperature coefficient. Its use has been mainly for pilot channel filters of rather narrow frequency bands.

6.3 Frequency Equations for Flexurel, Extensional and Shear Motions

In determining the motion and resonant frequencies of a particular type of vibrating system it is customary to consider an isolated type of motion in order that the solution shall be in a simple enough form to be practical even though it may not be too accurate. The more accurate type of solution is often so complex that its use for practical solutions might be small. Since any solutions so far obtained are not complete in every detail, it is usually necessary to resort to experimentally determined frequencies in any case, and the solution can only be regarded as a guide to the complete result. In the following treatment it will be assumed that the frequency equations are given for isolated modes of motion and it will be later shown which of these forms are coupled and the effect of the coupling.

6.31 Flexural Resonant Frequencies

The simplest equation relating the resonant frequencies of a rod vibrating in flexure is given by[1]

$$f = \frac{m^2}{2\pi}\frac{k}{\ell^2}\nu \qquad 6.1$$

where ν = velocity of extensional propagation $= \sqrt{Y_0/\rho}$
k = radius of gyration of cross section
Y_0 = Youngs modulus
ℓ = length
$m \doteq (n + 1/2)\pi$ for free-free modes
$\doteq (n - 1/2)\pi$ for clamp-free modes ($n > 1$)
n = order of mode (1, 2, 3, etc.)

This equation holds only for the case of a long thin rod. Measurements of the resonant frequencies of a quartz crystal vibrating with both ends free has shown the above equation to be true where m is defined approximately as $(n + 1/2)\pi$ provided $\frac{nw}{\ell}$ is less than .1. For values greater than this the measured values are somewhat lower than that predicted. When the dimension in the direction of vibration is appreciable in comparison with the

[1] Rayleigh, Theory of Sound, Vol. 1, Chapter VIII.

length, Mason[2] has shown that it is necessary to consider the effects of rotary and lateral inertia. His solution leads to the same frequency equation as 6.1 but with a different evaluation of the factor m which is obtained from the transcendental equations

$$\left.\begin{aligned} \tan m X &= K \tanh mX' \text{ for even modes} \\ \tan m X &= -\frac{1}{K} \tanh mX' \text{ for odd modes} \end{aligned}\right\} \qquad 6.2$$

where

$$X = 1/2\left[\left(1 + \frac{m^4 k^4}{4\ell^4}\right)^{1/2} + \frac{m^2 k^2}{2\ell^2}\right]^{1/2}$$

$$X' = 1/2\left[\left(1 + \frac{m^4 k^4}{4\ell^4}\right)^{1/2} - \frac{m^2 k^2}{2\ell^2}\right]^{1/2}$$

$$K = \left[\left(1 + \frac{m^4 k^4}{4\ell^4}\right)^{1/2} + \frac{m^2 k^2}{2\ell^2}\right]^2 \frac{X'}{X}$$

Equation 6.2 holds only for the case of a rod free to vibrate on both ends. The case of a clamp-free rod is somewhat more complicated since it cannot be given by separate solutions for the even and odd modes. The interpretation of m given in equations 6.2 will result in the same value as before [$m = (n + \frac{1}{2})\pi$] for values of $\frac{nw}{\ell}$ less than .05 but decrease considerably for larger values and ultimately as the bar becomes wider the effects of rotary inertia result in the flexure frequency approaching the extensional mode as an asymptote. As stated before measurements on quartz bars vibrating in flexure departed from that predicted by the simple definition of m when the width of the bar was such that $\frac{nw}{\ell} > .1$. By using the value of m defined by equation 6.2 it is possible to predict the frequency for widths as great as $\frac{nw}{\ell} = .5$. For widths greater than this, experiment shows a frequency lower than that predicted by equation 6.2. This then leads one to believe that the effect of shear plays an important part in the flexure of bars with appreciable width. An investigation of the effect of shear on the flexure frequencies of beams has been made by Jacobsen[3] and his results lead to the same frequency equation as 6.1 and to the same transcendental equations derived by Mason (6.2) but with different values of X, X' and K to account for the shearing

[2] W. P. Mason, "Electromechanical Transducers and Wave Filters," Appendix A. D. Van Nostrand Company, Inc.

[3] *Jour. Applied Mechanics*, March 1938.

effect. These values are given by

$$X = \frac{1}{2}\left[\left(1 + \frac{m^4 k^4}{4\ell^4}\left(\frac{1}{c_{jj}s_{ii}} - 1\right)\right)^{\frac{1}{2}} + \frac{m^2 k^2}{2\ell^2}\left(\frac{1}{c_{jj}s_{ii}} + 1\right)\right]^{\frac{1}{2}}$$

$$X' = \frac{1}{2}\left[\left(1 + \frac{m^4 k^4}{4\ell^4}\left(\frac{1}{c_{jj}s_{ii}} - 1\right)\right)^{\frac{1}{2}} - \frac{m^2 k^2}{2\ell^2}\left(\frac{1}{c_{jj}s_{ij}} + 1\right)\right]^{\frac{1}{2}} \qquad 6.3$$

$$K = \left[\left(1 + \frac{m^4 k^4}{4\ell^4}\left(\frac{1}{c_{jj}s_{ii}} - 1\right)\right)^{\frac{1}{2}} + \frac{m^2 k^2}{2\ell^2}\left(\frac{1}{c_{jj}s_{ii}} - 1\right)\right]^2 \frac{X'}{X},$$

where c_{jj} is the shear constant in the plane of motion s_{ii} is the elastic constant in the direction of propagation. While it is true that these values will result in a lower value of m than those associated with equation 6.2 and hence fit the actual measured results more closely for bars wider than $\frac{nw}{\ell} = .5$, there is some doubt in the minds of various investigators as to the actual amount of correction necessary to apply to compensate for the shear. The solution of equation 6.2 using the constants of equation 6.3 is a lengthy process and could only be applied to a given orientation since the elastic constants vary with direction in quartz. While the results of Jacobsen's work are difficult to handle for intermediate values of $\frac{nw}{\ell}$ where the correction of rotary and lateral inertia do not fit the measured results it does imply that for large values of $\frac{nw}{\ell}$ that the flexure frequencies will be mainly a function of the length alone. Therefore when we are concerned with very high orders of flexure in plates such as the case of high frequency AT and BT shear crystals we may assume the interfering modes due to flexures will be essentially harmonic in nature. Restating the general problem of determining flexure frequencies in quartz rods or plates we may assume that the ratio of width to length is the controlling factor in deciding which method of attack is to be employed. For values of $\frac{nw}{\ell}$ less than .1 equation 6.1 will give quite accurate results. For values of $\frac{nw}{\ell}$ up to .5 equation 6.1, using the values of m determined by equation 6.2 will give satisfactory results. While the values of m determined by using equation 6.3 will give more accurate results for the range .4 to .6, it is not desirable to carry it further because, while 6.2 does take into consideration the effect of shear it does not account for coupling to the shear mode of motion. Hence for values of $\frac{nw}{\ell} > .6$

it is best to depend upon experimental measurements if accurate results are a factor.

6.32 *Extensional Frequencies*

The resonant frequencies of a bar vibrating along its length, commonly called an extensional mode of motion is derived quite easily from the wave equation in one dimension and is given by

$$f = \frac{n}{2\ell_i}\sqrt{\frac{1}{s_{ii}\rho}} \tag{6.4}$$

where ℓ = length
s_{ii} = elastic constant in the direction of propagation
ρ = density
n = 1, 2, 3, 4, etc.

This is the case when the length is the greatest dimension. When we consider extensional modes along the thickness of a plate, it can be shown that the c constants be employed to account for the lateral inertia in the two directions at right angles to the direction of propagation, (provided that the resulting motion is nearly along the thickness direction). Hence, for thin plates

$$f = \frac{n}{2\ell_i}\sqrt{\frac{c_{ii}}{\rho}} \tag{6.5}$$

As an example of the use of the above equation an X-cut bar vibrating along its length would result in a series of resonant frequencies defined by equation 6.4. An X-cut plate vibrating along its thickness would result in a series of frequencies defined by equation 6.5. Applying the appropriate constants

$$f_\ell = \frac{n}{2Y}\sqrt{\frac{10^{14}}{127.9 \times 2.65}}$$

$$= \frac{272}{Y(\text{cm})}\, n \quad \text{kilocycles} \tag{6.6}$$

and

$$f_t = \frac{n}{2X}\sqrt{\frac{86.05 \times 10^{10}}{2.65}}$$

$$= \frac{285}{X(\text{cm})}\, n \quad \text{kilocycles} \tag{6.7}$$

This shows that although Young's Modulus is the same in the two directions the resulting frequency constants are different because of the conditions at the boundaries.

6.33 *Shear Resonant Frequencies*

As shown in section 6.23 the low frequency face type shear mode results in a doubly infinite series of frequencies due to the manner in which the plate may break up into reversals of phase along its length and width. While a solution for the low frequency shear motion that satisfies the boundary condition of a free edge has not yet been accomplished, several approximate solutions for the frequencies are available. A modification of the equation developed by Mason[4] will give results which verify experimental data.

$$f = \frac{1}{2}\sqrt{\frac{1}{\rho s_{ij}}}\sqrt{\frac{m^2}{\ell^2} + k^2\frac{n^2}{w^2}} \qquad 6.8$$

where ρ = density
s_{ij} = shear modulus in ℓw plane
m, n = 1, 2, 3, etc.
ℓ = length of plate
w = width of plate

The value of k so far remains experimental and for low orders of m and n may be assumed unity. Its use is mainly for high orders of m and n where Young's modulus is different in the ℓ and w directions. Experimental data in the case of BT plates indicates that it should be 1.036 to account for the difference in velocity in the two directions. When m or n is large the velocity component, namely $\sqrt{\frac{1}{\rho s_{ij}}}$ should be replaced by $\sqrt{\frac{c_{ij}}{\rho}}$ for reasons explained for the extensional case. Equation 6.8 holds for the case of a plate vibrating in low frequency shear in regions where no highly coupled extensional or flexural resonant frequencies exist. As will be shown later, these regions are few. By assuming the frequencies are given by these equations and then applying the normal correction for coupled modes, a fairly accurate result will be obtained.

The high frequency case of a plate vibrating in shear is somewhat similar to the face shear or low frequency case with the exception that three dimensions must be considered since two are large compared to the third (the main frequency controlling dimension). An experimental formula for this case is given by

$$f = \frac{1}{2}\sqrt{\frac{c_{ij}}{\rho}}\sqrt{\frac{m^2}{t^2} + k\frac{n^2}{\ell^2} + k_1\frac{(p-1)^2}{w^2}} \qquad 6.9$$

where c_{ij} = shear modulus in plane of motion
ρ = density
ℓ, w, t = length, width and thickness

[4] "Electrical Wave Filters Employing Quartz Crystals as Elements," W. P. Mason, *B.S.T.J.* July, 1934.

m, n and p represent reversals of phase along the three directions and may be termed overtones. The values of k and k_1 are inserted to correct for the change in shear velocity resulting from a change in Young's modulus in the three directions. For most work with oscillator crystals where the length and width are large compared to the thickness, the following simplification of equation 6.9 is most useful.

$$f = \frac{m}{2t}\sqrt{\frac{c_{ij}}{\rho}} \qquad 6.10$$

When high frequency shear type crystals are used in connection with selective networks, it is necessary to make use of equation 6.9 to determine where the next possible pass regions will occur.

6.34 *Effects of Rotation About the Crystallographic Axes on the Resonant Frequencies and Coupling between Modes of Motion*

Several of the elastic constants have been used in equations expressing the resonant frequencies. Since most of the crystal cuts now in use are rotated at some particular angle about the X crystallographic axis, it is of interest to know the effect of this rotation upon the elastic constants since they determine the resonant frequencies and the coupling between certain of the modes of motion. The general stress-strain equations for an aeolotropic body are given in equation A.1 of Appendix A together with their definitions. In the case of quartz where the axes of the finished plate are aligned with the crystallographic axes the constants reduce to 7 and are shown in equation A.8. Examination of these equations shows that there are extensional and shearing strains resulting from dissimilar extensional and shearing stresses through the elastic constants s_{ij} and c_{ij}. This results in coupling between modes of motion where a so-called cross strain exists. These couplings may be made zero or small by proper orientation of the crystal plate about the X crystallographic axis. The mathematics of this operation is simplified by the use of matrix algebra[5]. Upon performing this operation a new set of elastic constants are obtained and are plotted graphically together with the piezoelectric constants on Fig. 6.7. From this figure we may see that the coupling resulting from the s'_{24} constant will be zero if the crystal plate is orientated by $-18.5°$ about X with respect to the crystallographic axis. This constant determines the coupling between the extensional mode along the length (Y' dimension) and the face shear mode ($Y'X'$ dimensions). This analysis resulted in the use of the $-18.5°$ cut in the channel filters of the coaxial system. Two other crystal cuts resulting in low coupling between different modes of motion are the AC and

[5] "The Mathematics of the Physical Properties of Crystals," W. L. Bond, *B.S.T.J.*, Jan. 1943.

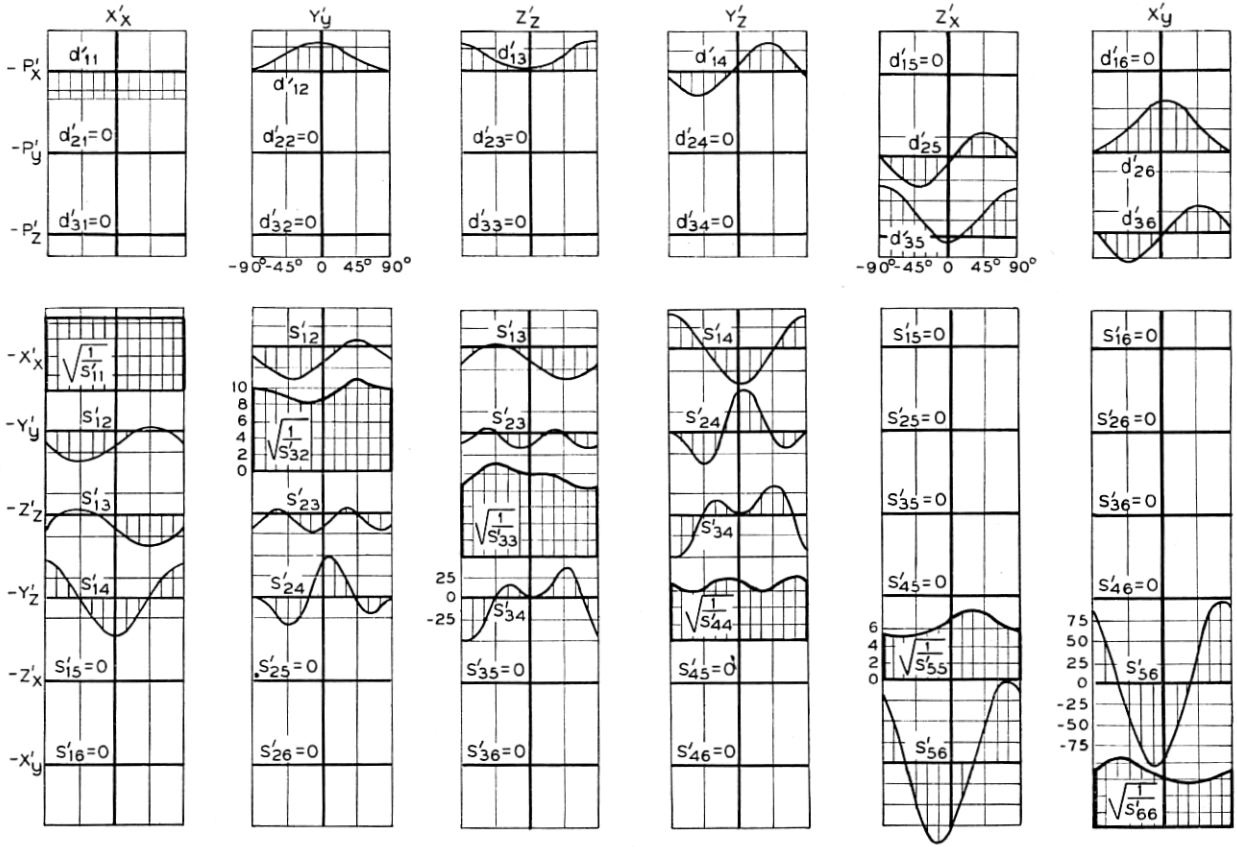

Fig. 6.7—Variation of piezo electric and elastic constants of quartz with rotation about the X crystallographic axis.

BC cuts. The s'_{56} constant determines the coupling between the face and thickness shear modes. As shown in Fig. 6.7 this constant passes through zero at two values, namely $+31°$ and $-59°$ and the resulting angles have been termed the *AC* and *BC* cuts. These angles are very close to the *AT* and *BT* cuts and hence they also possess the benefits of low coupling between modes. In addition to making the cross coupling constants zero, a rotation of the crystal plate with respect to the crystallographic axes also results in a change in the extensional and shear elastic constants. Notice that these pass through maxima and minima at the zero values for the cross coupling constants. This of course affects the resonant frequencies of isolated modes. Changes as great as 50% increase in frequency constants may be obtained by choosing the proper rotations. The equations relating the elastic constants as functions of orientation are given in appendix B for more complete use.

6.4 Coupling between Modes of Motion

As pointed out in the previous section, the frequency equation of a given mode of motion will give accurate results only in the case where the mode of motion is isolated. This is very rarely the case since most quartz crystals in common use are in the form of plates where the frequency determining dimension is not large in comparison with all other dimensions. Only in the case of a long thin rod vibrating in length-thickness flexure of the first order would this be true. It was also shown that the coupling between different modes of motion could be related to the mutual elastic constants (s_{ij} and c_{ij}) and that some of these could be made zero by the proper choice of orientation of the finished crystal plate. The elastic constants s_{ij} and c_{ij} only relate to the coupling between the extensionals, the shears and the extensional to the shear. For example s_{23} relates to the coupling between the extensional modes along the *Y* and *Z* axes, s_{56} relates to the coupling between the low and high frequency shear modes of a *Y* cut plate and s_{24} relates to the coupling between an extensional mode along the *Y* axis and a shear mode in the *YZ* plane. One other important coupling condition occurs and that is between the flexure and the shear modes. There is at present no mathematical theory relating this form of coupling except from simple assumptions that may be drawn from the fact that the shear modulus enters as a controlling factor in determining the frequency of a bar vibrating in flexure and from the similarity of the two types of motion near the boundaries. Since it is possible to have a definite coupling between extensional and shear modes there must be coupling between the extensional and flexure modes. It would be expected that it would be proportional to the coupling between the extensional and shear modes.

6.41 *Extensional to Shear and Extensional to Flexure Coupling*

The coupling between the extensional and shear motion can best be illustrated by taking the case of an X cut plate the length of which lies along the Y axis and the width along the Z axis. This is shown in Fig. 6.8 together with two other cases, one in which the plate is rotated about the X axis by $-18°$ and the other a similar rotation but $+18°$. Also in Fig. 6.8 is shown an enlarged view of the change in the elastic constants and frequency constants as a function of the rotation of the plate about the electric or X axis. For the case of an X cut plate the strains resulting from an applied exten-

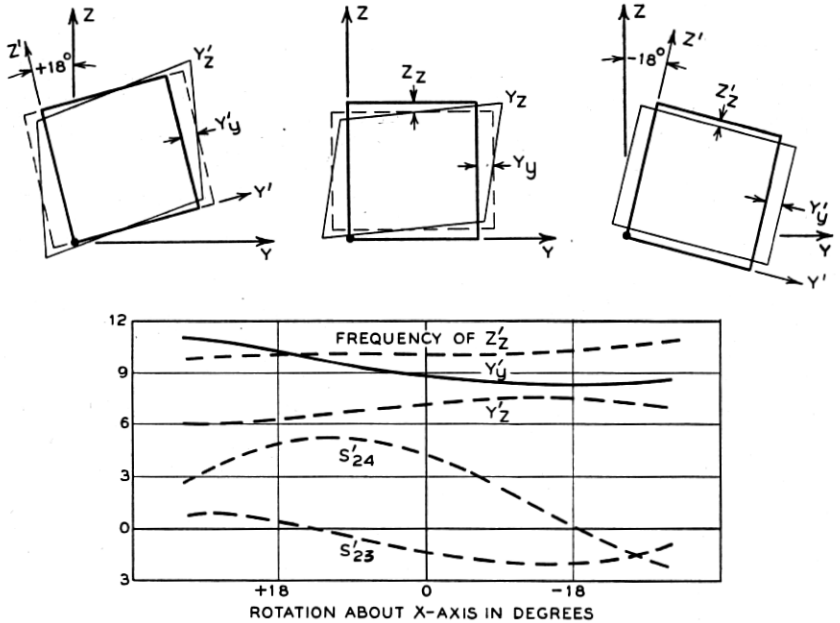

Fig. 6.8—Motion in an X cut plate for different orientation about the X crystallographic axis.

sional stress along the length according to equation A.8 would be

$$\begin{aligned} x_x &= s'_{12}\, Y_y \\ y_y &= s'_{22}\, Y_y \\ z_z &= s'_{23}\, Y_y \\ y_z &= s'_{24}\, Y_y \end{aligned} \qquad 6.11$$

where x_x is an extensional strain along the thickness
y_y " " " " " " " length
z_z " " " " " " " width
y_z " a shear strain in the length-width plane

If the plate is thin we may neglect the x_x strain as far as its effect on the resonant frequencies associated with the length and width are concerned. From the plot of the elastic constants on Fig. 6.8 we may determine the strains resulting from a stress along the length of an X cut plate for various orientations about the X axis. In addition to the expected extension along the length we have for a $+18°$ cut, a large amount of length-width or y'_z shear strain due to s'_{24} and very little width or z'_z strain. For the 0° cut there is also large length-width or y'_z shear strain and a width or z'_z strain. In the case of the $-18°$ cut the shear strain vanishes due to s'_{24} being zero, leaving in addition to the expected length or y'_y strain a width or z'_z strain. These relationships are more clearly shown if we plot the resonant frequencies resulting from the three modes of motion namely, the extensional modes along the length and width and the shear mode in the length-width plane

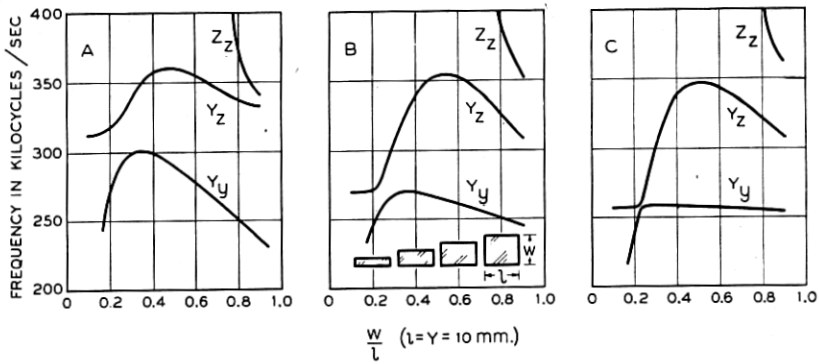

Fig. 6.9—Effect of rotation about the X axis on the resonant frequencies of an X cut plate.

A plot of measured resonances is shown in Fig. 6.9 for the above described three cases as a function of the change in width. The resonant frequencies for these three types of motion are given in section 6.3 as

$$f_{y'_y} = \frac{1}{2\ell}\sqrt{\frac{1}{\rho s'_{22}}}, \text{ extensional along } \ell \qquad 6.12$$

$$f_{z'_z} = \frac{1}{2w}\sqrt{\frac{1}{\rho s'_{33}}}, \text{ extensional along } w \qquad 6.13$$

$$f_{y'_z} = \frac{1}{2}\sqrt{\frac{1}{\rho s'_{44}}}\sqrt{\frac{1}{\ell^2}+\frac{1}{w^2}}, \text{ shear in } \ell w \text{ plane} \qquad 6.14$$

These equations specify only the uncoupled modes and do not take into consideration the effect of coupling to other modes of motion. In the case of Fig. 6.9 it is shown that when only the width is changed the extensional

mode along the length (the y'_y mode) is unaffected only in the case of the $-18°$ cut. The effect of coupling between the extensional and shear is clearly shown in the case of the 0° cut by the change in the length-extensional frequency. This is more pronounced in the $+18°$ case not because of more coupling but because the frequency constants of the two modes are more nearly alike as indicated in Fig. 6.8.

The mode of motion associated with the line intersecting the extensional y'_y mode is that due to the second length-width flexure mode. As mentioned before it is strongly coupled to the shear mode in the same plane. The coupling between this flexure and the extensional mode is directly related to the coupling between the shear and the extensional mode. This is borne out by Fig. 6.9, for in the case of the $-18°$ cut, s'_{24} is zero and as can be seen the change in frequency of the extensional mode is very slight even when the flexure mode is nearly identical in frequency.

We may state generally that the change in frequency of a particular mode of motion from that of its uncoupled state is dependant on two factors; the coupling to and the proximity to other forms of motion. This follows well established mathematical procedures but to solve the case just discussed would require the solution of a four mesh network with mutual impedances the values of some of which are at best only approximate. This will serve to illustrate that the use of formulae such as given in section 6.3 may be used more as a guide in establishing certain modes of motion rather than for accurate determinations of resonant frequencies.

6.42 *Flexure to Shear Coupling*

1. *Low Frequency Shear*

As previously indicated there is no simple means of mathematically determining the coupling between flexure and shear types of motion as there is between the extensional and extensional to shear modes. Here we must base our assumptions upon observed experimental evidence and simple reasoning. The relation between flexure motion and shear motion can be illustrated by the figures associated with Fig. 6.10. The forces that are necessary to produce flexure and shear motion are shown by arrows in Fig. 6.10. When the two arrows point toward each other, it indicates a compression and when the arrows point away from each other, it indicates tension. The diagrams on the left of Fig. 6.10 illustrate the conditions for flexure motion and the diagrams on the right indicate the conditions for shear motion. Notice that in the case of the first flexure and the second shear that the forces applied to the top and bottom of the plate are similar. Also in the case of the second flexure and third shear, they are similar. Here again we have certain similarities which in this case are important to remember.

The motion of the ends of the plate in the case of the first flexure are similar to those of the second shear. In the case of the second flexure the similarity is observed in the case of the third shear. The end motion in the case of the third shear is also the same in the case of the first or any odd shear. Likewise, the end motion of the first flexure is similar to the second shear or any even shear. We may then generalize and say that it is very likely that an odd order flexure would be coupled to an even shear; and also an even flexure would be coupled to an odd shear.

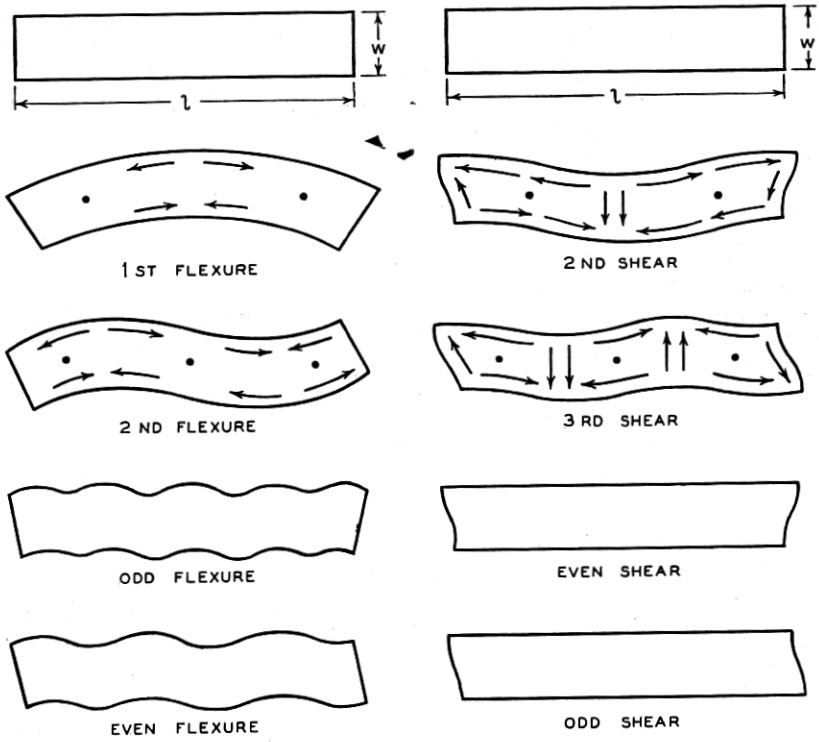

Fig. 6.10—Similarities in shear and flexure motions in a bar.

To illustrate the coupling between flexure and shear type motions, the frequencies of flexure and shear modes in a Z-cut quartz plate as shown in Fig. 6.11 have been measured. These measured frequencies are shown by the solid lines for various widths of the plate. It will be seen that there are no observed resonances following an unbroken continuous line to represent the shear frequency, but they are interrupted by several other frequencies which we must interpret as being various even modes of the flexure in the plane of the plate. It is clearly shown here that only even order flexures are

strongly coupled to the fundamental or odd shear. The strong coupling shown between the X_y shear and the second X_y flexure explains why the frequency equations given in section 6.3 for the frequency of flexure and

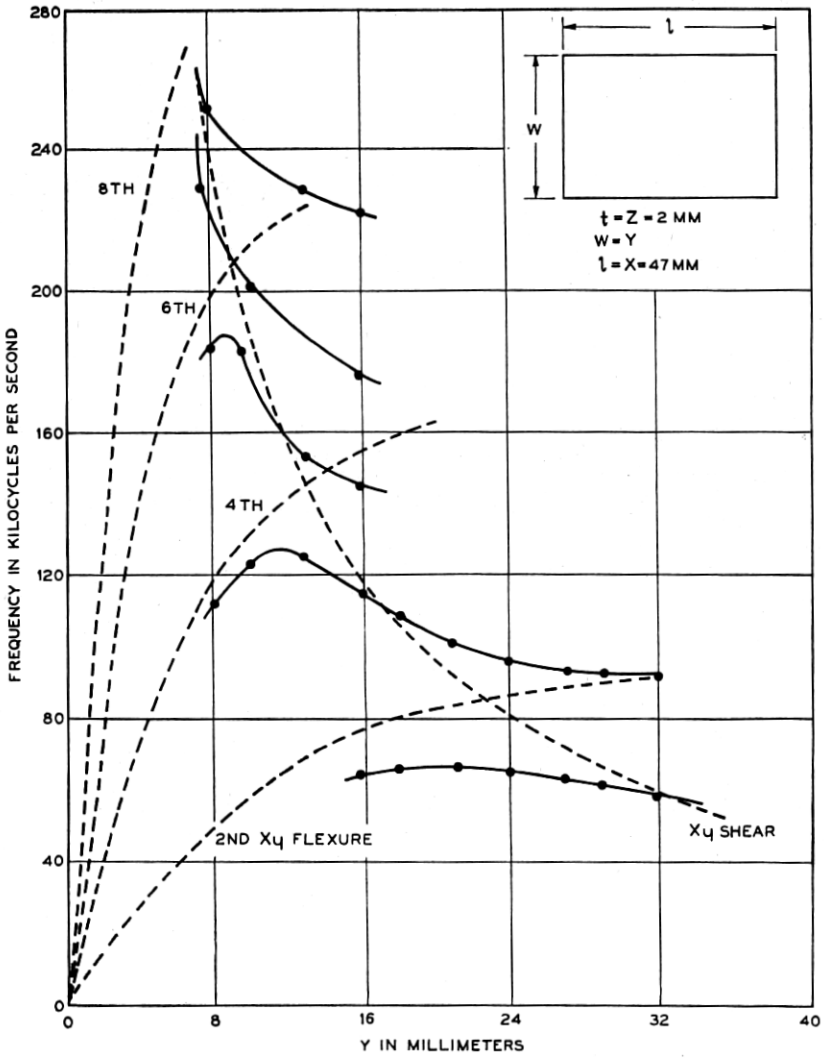

Fig. 6.11—Shear and flexure resonances in a Z-cut quartz plate.

shear modes will not give even approximate results if applied to this case for a square crystal. It will be shown later that if account is taken of coupling, the shear mode for a square crystal of this type may be more accu-

rately determined. Fig. 6.12 is a more detailed representation of the conditions shown broadly in Fig. 6.11 except in this case an AC-cut quartz plate was used and most of the observable resonant frequencies are shown

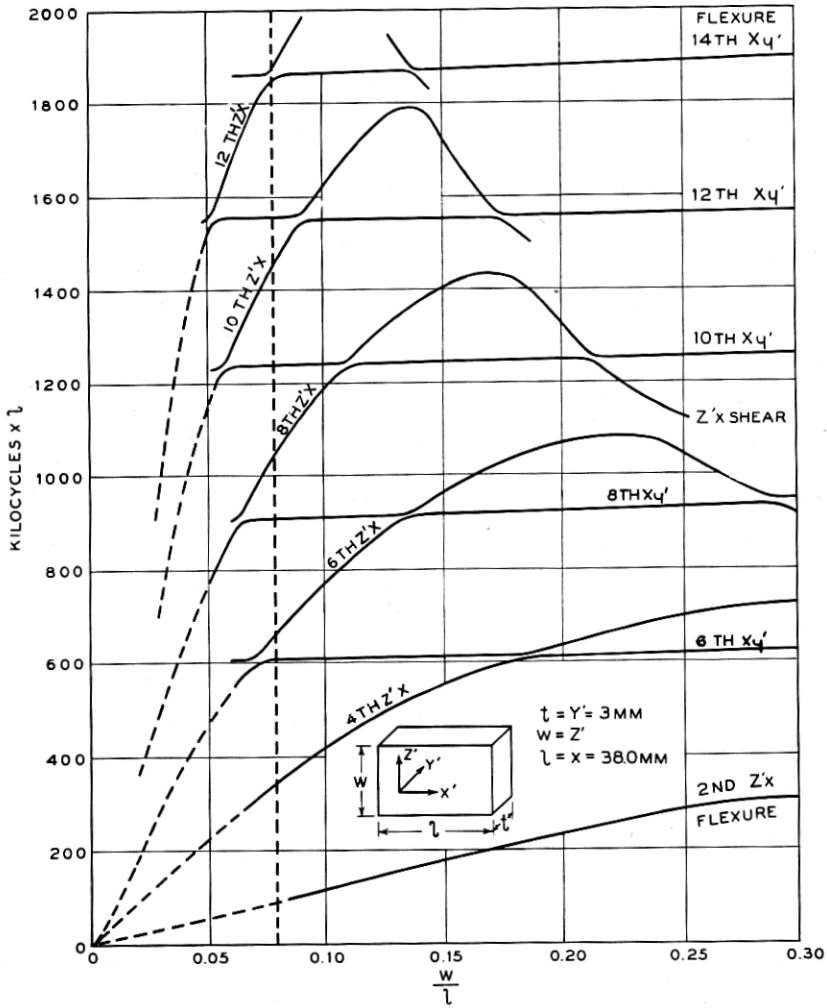

Fig. 6.12—Shear and flexure resonances in an AC-cut quartz plate.

for various values of $\frac{w}{\ell}$. The plate shear is labeled Z'_x shear and occurs at the frequencies predicted by equation 6.8 except in the regions where a flexure in the same plane exists. This is the type of motion shown in Fig. 6.4 for the case of $m = 1$, $n = 1$. It can be seen that as the difference in order of modes becomes greater the effect on the shear frequency is less

except where they are coexistant. We can then state generally that even though there is coupling between particular modes of motion, if the difference in order is great, the approximate frequencies may be computed as though they were isolated. This is more clearly shown in the case of thickness shear modes. The modes that are shown coupled to the face shear mode are Z'_x flexures propagated in the direction of the length or X axis. The lower orders can be shown to follow the general frequency equation discussed in section 6.3 but the higher orders for a given $\frac{w}{\ell}$, it will be noticed, are regularly spaced in frequency and show the effect of shear. The X'_y flexure modes determined by the length and thickness are shown as nearly horizontal lines since only the width was changed. Since these two groups of flexure modes are propagated in the same direction, it would be expected that the difference in frequency for the same ratio of dimension $\left(\text{i.e., } \frac{w}{\ell} = \frac{t}{\ell}\right)$ would be due to the differences of the shear coefficients in the two planes of motion. The vertical dotted line indicates the ratio of thickness to length. When the ratio of width to length is equal to this value it can be seen that the flexure modes in the width-length plane are in all cases higher than the same order flexures in the thickness-length plane. An examination of Fig. 6.7 shows that for an AC-cut crystal the shear modulus in the width-length plane $\left(\frac{1}{\sqrt{s'_{55}}}\right)$ is greater than that in the thickness-length plane $\left(\frac{1}{\sqrt{s'_{66}}}\right)$. This is in agreement with the observation made above. One other generality may be drawn from the experimental data shown in Fig. 6.12. The coupling between flexure modes and shear modes in planes at right angles to each other is very small in comparison with that between modes in the same plane.

As mentioned before the effect of coupling between modes of motion is greatest when the orders are more nearly similar. In this particular crystal this effect can be shown between the fundamental width-length Z'_x shear and the second order width-length Z'_x flexure. This is shown in Fig. 6.13 which is an extension of the data shown in Fig. 6.12 for a crystal nearly square and shows the frequency range covered only by the second flexure and the fundamental plate shear. A computation of the uncoupled second flexure mode propagated along the length and the first plate shear mode are shown by the solid lines f_f and f_s respectively. Inserting the appropriate constants the formulae of section 6.3 become

$$f_f = \frac{1}{2\pi}\sqrt{\frac{7.85 \times 10^{11}}{12 \times 2.65}}\, m^2 \frac{Z'}{X^2} \qquad 6.15$$

$$f_s = \frac{1}{2}\sqrt{\frac{71.8 \times 10^{10}}{2.65}}\sqrt{\frac{1}{X^2} + \frac{1}{Z'^2}} \qquad 6.16$$

In evaluating m, account was taken only of the rotary and lateral inertia so that some error is expected at the larger ratio of axes. The curve of flexure crosses the shear curve at $\frac{w}{\ell} = .76$, a condition which we know to be non-compatible since these two motions are coupled. From the theory of coupled circuits we can determine the displacement of two uncoupled frequencies as a result of the coupling, through the relation

$$f_{1,2}^2 = \tfrac{1}{2}[f_s^2 + f_f^2 \pm \sqrt{(f_s^2 - f_f^2)^2 + 4k^2 f_s^2 f_f^2}] \qquad 6.17$$

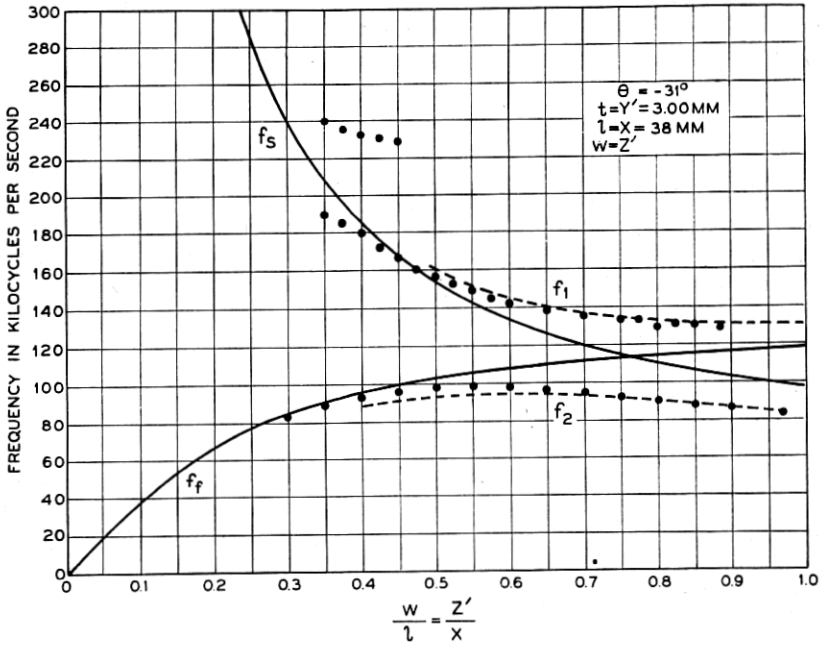

Fig. 6.13—Effect of coupling on the plate shear and the second flexure mode in an *AC*-cut quartz plate.

where f_s = uncoupled shear frequency,
f_f = " flexure "
k = coefficient of coupling.

The coefficient of coupling in this case may be defined as the ratio of the mutual to the square root of the self compliances of the two vibrating systems. As mentioned before no derivation has yet been made to indicate the relation between the coupling between these two forms of motion and the physical constants of the medium in which the vibration occurs. It is necessary to assume some coupling factor which will produce that observed

by experiment. Applying a coupling coefficient of 35% and computing the values of f_1 and f_2 from equation 6.17 the results are the dotted curves shown in Fig. 6.13. The observed points follow the computed values to a fair degree of accuracy for all frequencies below 180 kilocycles. Above this range there is a strong coupling to the fourth flexure and this would require separate consideration. Based upon these results the equation for the low frequency or face shear given in section 6.3 would not give the observed results for a nearly square plate because of the high coupling to the second flexure mode. For an approximately square plate, cut near the *AC*-cut the plate shear frequency including the effect of coupling would be given by

$$f = \frac{.849\sqrt{2}}{2d}\sqrt{\frac{1}{\rho s'_{55}}}, \qquad 6.18$$

where

$$d = \tfrac{1}{2}(X + Z')$$

and .849 is the factor resulting from the use of equation 6.17. For crystal cuts far different from the above it would be necessary to consider the flexure and shear as uncoupled and then apply equation 6.17 to determine the appropriate factor for square plates.

2. *High Frequency Shear*

The motion associated with flexure has been shown in Fig. 6.1 and in order to determine the frequency of higher order flexures, measurements were made on an *AC*-cut crystal. The results of these measurements are shown in Fig. 6.12. The first flexure motion to be expected with this crystal would be a flexure in the plane of the length and width. The various orders of these flexures are shown by the curved lines labeled second z'_x fourth, sixth, etc., all radiating from zero frequency (Primed values of z and y indicate that these are not crystallographic axes). The equation commonly determining the frequency of flexure states that the frequency should be proportional to the width and inversely proportional to the square of the length. If this were true, these curved lines representing the resonances of this type flexure shown on Fig. 6.12 would then be straight lines. Since the actual conditions show a wide departure from this, we must assume that this departure is due to rotary and lateral inertia and the effects of shear. It will be noticed that as we progressively increase the order of the harmonic, that the actual frequency spacing for a given value of $\frac{w}{\ell}$ is very nearly linear instead of a square law. This point is more clearly seen when we examine the frequency of higher orders of the flexures in the length thickness or xy' plane. As shown on Fig. 6.12 these frequencies

labeled 6th x_v, etc., change very little and are nearly horizontal straight lines. Here again they appear to be simple harmonics of some common low frequency. Also it will be noted that the coupling between the z_x' flexures and the z_x' shear is quite appreciable and in general decreases as the difference in order of the two modes becomes greater. This plot of the various flexure frequencies tells us a great deal about the behavior of progressively higher order of flexure type motion. The important effect to be noticed is that for high orders, and a fixed ratio of $\frac{w}{\ell}$, the flexure may be treated as though it were harmonic so far as frequency is concerned. Some variations to this rule will be observed and special cases will be discussed. So far we have discussed the case of flexure modes of relatively low order. In the case of high frequency shear modes of motion, we would expect that the order of flexure which would interfere with this type of motion would be rather high.

Figure 6.14 shows a plot of these flexure modes as observed in an AT-cut plate. These are shown by dashed lines. The dots indicate actual measured resonances. This figure also shows the various other resonant frequencies observed in this type of plate as discussed in section 6.2. The solid lines labeled mnp represent the type of shear motion shown in Fig. 6.5. Here again we may observe certain statements made before with respect to the coupling between shear and flexure type motions. Notice in this case that the coupling between an even order flexure and an odd order shear is high and increases as the orders more nearly approach each other. For example, the 38th flexure mode is coupled to the fundamental shear labeled $m_1n_1p_1$ has very little coupling to the second order shear $m_1n_2p_1$, and again is strongly coupled to the third shear $m_1n_3p_1$ and correspondingly higher coupling to the fifth shear. When we speak of higher order shears, such as $n_2n_3n_5$, they are not higher order in the sense of harmonics, but do differ by a small amount in frequency. In the case of a plate where ℓ is not great compared to t, these differences will be greater.

In actual practice in the case of AT plates, we are usually concerned mainly with the fundamental high frequency shear and high even order flexures along the length. This case is shown in Fig. 6.15 which gives experimental results of measurements on actual AT plates. It will be noticed that the flexure frequencies show a rather regular displacement as the ratio of the length of the plate to its thickness is changed. In this case only the odd order modes of shear and the even modes of flexure are shown. It will be observed that as the ratio of the length to thickness decreases, the coupling between these modes is quite high. This some state of affairs is illustrated again in the case of the third harmonic of high frequency shear and is shown in Fig. 6.16. The near vertical dashed lines represent even order

flexure frequencies and the curve labeled m_3n_1 and the curve labeled m_3n_3 correspond to two different values of the high frequency shear near its commonly called third harmonic.

An examination of Figs. 6.14 and 6.15 indicates that a regular pattern is formed of the ratios of axes at which the high frequency shear and succes-

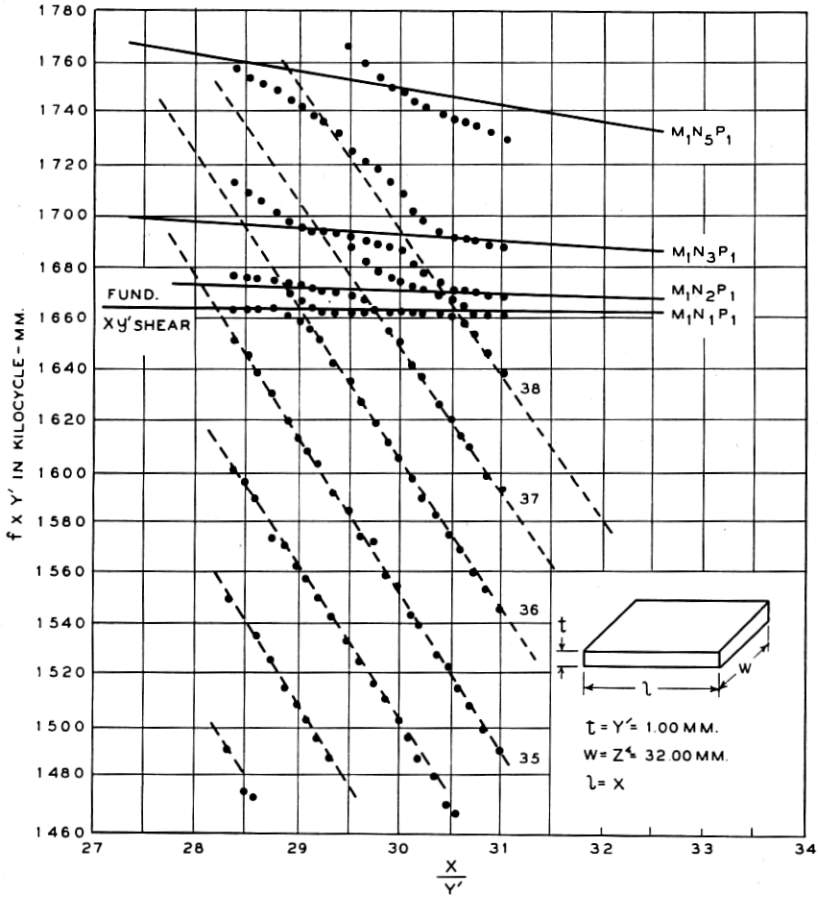

Fig. 6.14—High frequency flexure and shear resonances in an AT-cut quartz plate.

sive even orders of the length-thickness flexure coincide. Rather than define these points on the basis of specific ratios of axes it is more convenient to place them on a frequency basis. Therefore we may say that for a given size plate there will be specific frequencies at which some mode of the flexure motion along the length will be the same as the high frequency thickness

shear. For the case of AT plates experiment has shown these to be given by

$$f_{xf} = \frac{1338.4}{X} n_{xf}, \quad \text{kilocycles} \qquad 6.19$$

where X = length of X axis in millimeters,
n_{xf} = order of flexure along X axis
= 1, 2, 3, 4, etc.

In this equation as well as those of a similar nature to follow it is assumed that the thickness is such as to result in the same frequency for the high

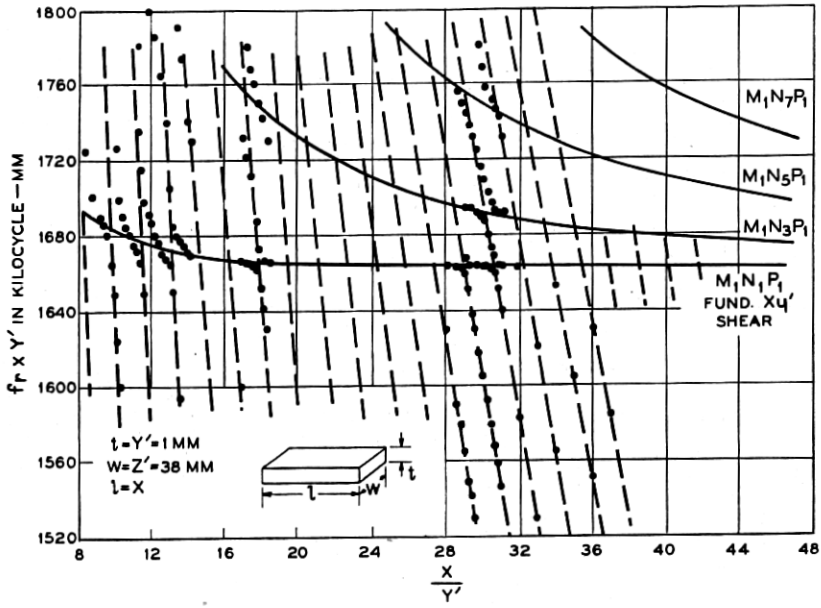

Fig. 6.15—High frequency flexure and shear resonances in an AT-cut quartz plate.

frequency X_y shear mode. As shown in Fig. 6.14 only the even orders are strongly coupled to the fundamental thickness shear.

The coupling between high even orders of the flexure along the X axis and the high frequency shear in the case of BT-cut plates is similar to that for AT-cut plates. Fig. 6.17 shows the various resonant frequencies observed in a BT-cut crystal as a result of changing the ratio of the length or X axis to the thickness or Y' axis. The curve m_1n_1 represents the high frequency X_y, shear. Curves m_1n_3, m_1n_5, m_1n_7 and m_1n_9 represent other X_y, shear modes as discussed in section 6.23 resulting from higher orders along the length or X axis. The dashed lines represent even order flexure modes along the X axis. The same regularity is observed here as in the case of the

AT-cut. When placed on a frequency rather than a ratio of axis basis the frequencies at which flexure modes along the X axis would coincide with the

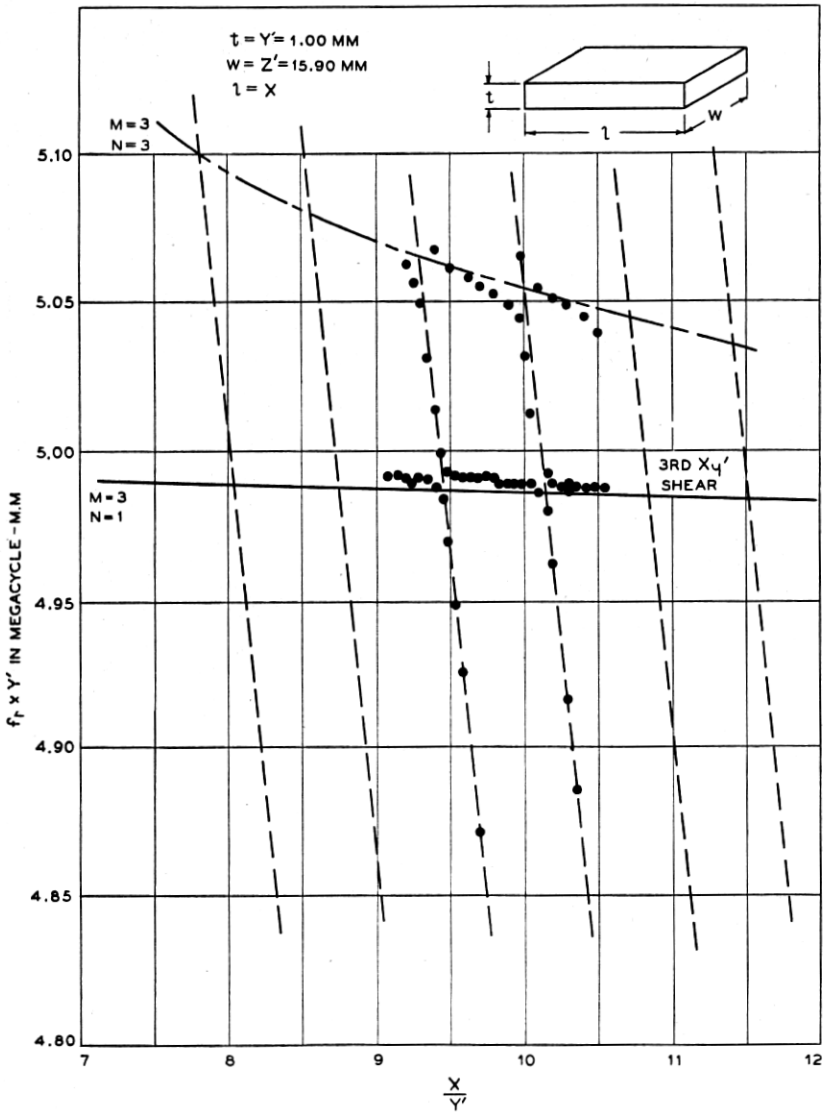

Fig. 6.16—High frequency flexure and shear resonances in an AT-cut quartz plate near the third harmonic shear mode.

fundamental $X_{y'}$ shear mode are experimentally given by

$$f_{xf} = \frac{1818}{X} n_{xf} \quad \text{kilocycles} \qquad 6.20$$

where X is given in millimeters. In this case it will be noticed also that only even order flexures are strongly coupled to the fundamental $X_{y'}$ shear.

The dependence of the flexure frequency on the shear coefficient can be seen from these two cases. The direction of propagation is the same in both cases (along the X axis) but the direction of particle motion is nearly at right angles. It would be expected then that the frequency constant would be highest for the case of the highest shear coefficient. Examination of equa-

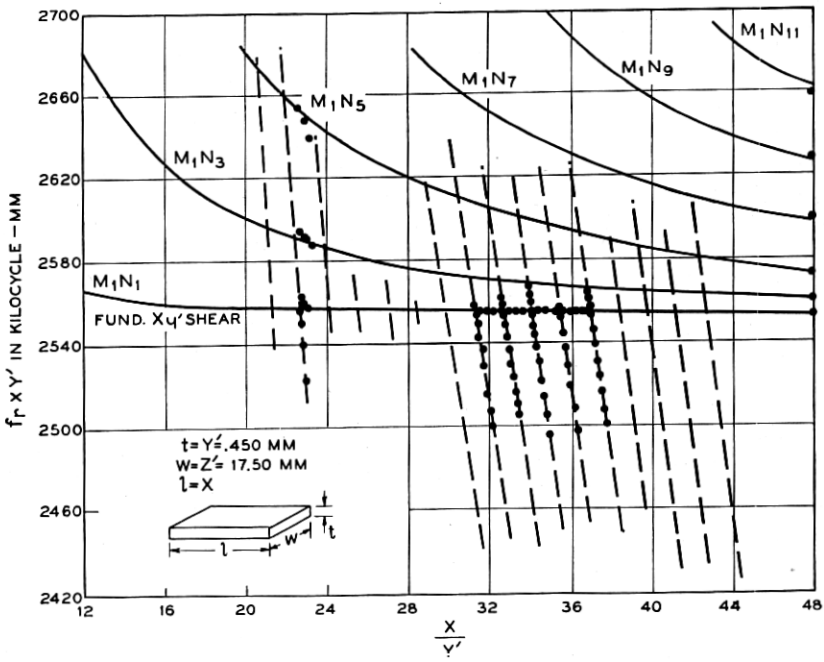

Fig. 6.17—High frequency flexure and shear resonances in a BT-cut quartz plate.

tions 6.19 and 6.20 shows this to be true. In addition, the change in the frequency constant is about the order of magnitude of the change in the shear modulus in the respective planes of motion.

6.43 *Coupling between Low Frequency Shear and High Frequency Shear*

From an examination of Fig. 6.7 it can be seen that the coupling between the low frequency shear (Z'_x) and the high frequency shear Xy' is related by the s'_{56} constant. In the AC and BC-cuts this reduces to zero but for the AT and BT-cuts it has a finite small value. According to section 6.3 the frequencies of the plate shear modes are given by equation 6.8 but this holds only for the case where m and n are small. When the third dimension

becomes appreciable in comparison with a half wave length along w or l it becomes necessary to use the c constants. When considering high orders of the low frequency shear equation 6.8 is modified to

$$f = \frac{1}{2}\sqrt{\frac{c_{jj}}{\rho}}\sqrt{\frac{m^2}{l^2} + k^2\frac{n^2}{w^2}} \qquad 6.21$$

Equation 6.21 shows that high orders of the low frequency or plate shear are dependent upon both the length and width dimensions and it might be assumed that this would lead to very complicated results in so far as analysis of experimental data is concerned. The coupling between these modes and the high frequency shear is a result of coupling in the mechanical as well as

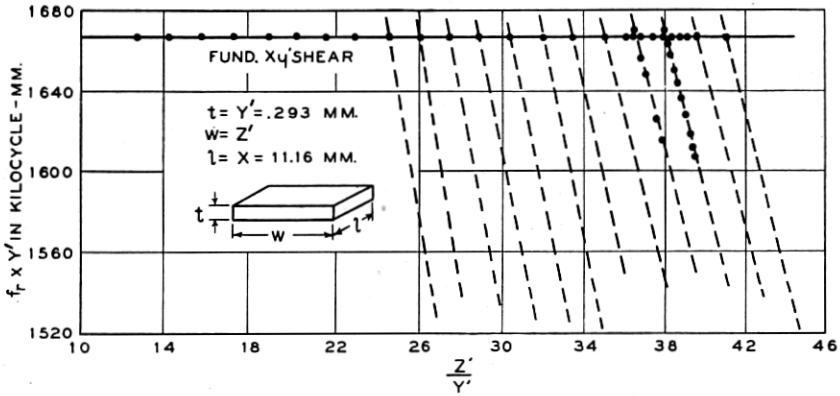

Fig. 6.18—High frequency shear resonances in an AT-cut plate.

the electrical systems. The strongest coupling with reference to the length axis would then be for high odd orders of m and unity for n with successively smaller coupling for higher orders for n if the driving potential extends over the complete surface of the crystal. In a similar manner when considering high orders of plate shear along the width axis the highest coupling will result from unit order for m. Based on these assumptions then to a first approximation we can assume these modes to be functions of length and width alone. Equation 6.21 then reduces to

$$f_{l_s} = \frac{1}{2}\sqrt{\frac{c_{jj}}{\rho}}\frac{n_{l_s}}{1} \qquad 6.22$$

$$f_{w_s} = \frac{k}{2}\sqrt{\frac{c_{jj}}{\rho}}\frac{n_{w_s}}{w} \qquad 6.23$$

where n_{sl} = order of shear mode along l axis,
n_{sw} = order of shear mode along w axis.

These modes have been measured in AT and BT-cut crystals. Fig. 6.18 shows the points at which these modes intersect the fundamental high frequency shear mode in AT-cut plates. This is the case for high orders along the Z' or width axis. A similar set of resonances can be shown to exist when the X or length axis is varied. Experiment has shown that these frequencies of coincidence between high order plate shear modes and the fundamental high frequency $X_{y'}$ shear mode for the case of AT-cut plates is given by

$$f_{xs} = \frac{254.2}{X} n_{xs} \text{ kilocycles} \qquad 6.24$$

$$f_{z's} = \frac{254.0}{Z'} n_{z's} \text{ kilocycles} \qquad 6.25$$

where X and Z' are given in centimeters. Only odd orders are strongly coupled if the crystal plate has a symmetrical contour with respect to an applied equipotential electrode. Upon substitution of the value of c'_{55} for an AT-cut crystal in equation 6.22 there results

$$f_s \times \ell = \frac{1}{2}\sqrt{\frac{c'_{55}}{\rho}} = \frac{1}{2}\sqrt{\frac{67 \times 10^{10}}{2.65}} = 251.0 \text{ kilocycle} - \text{cm.} \qquad 6.26$$

which is within 1 per cent of that found experimentally. Since Young's modulus is nearly the same along the X and Z' axis the value of k in equation 6.23 is essentially unity. Fig. 6.19 shows measured values of high order Z'_x shear modes near the high frequency $X_{y'}$ shear mode in a BT-cut crystal for various values of the width or Z' axis. More detailed measurements have been made of the high order Z'_x plate shear modes in BT-cut plates along the X axis. Fig. 6.20 shows both the shear and flexure modes along the X axis near the vicinity of the high frequency $X_{y'}$ shear mode. Since the frequency constant for the Z'_x shear modes is different from that for the $X_{y'}$ flexures there are regions where, if no coupling existed, all three modes would be at the same frequency. It is obvious from Fig. 6.20 that this is not the case. Therefore, we must assume that not only are the high order Z'_x shears and $X_{y'}$ flexures coupled to the high frequency $X_{y'}$ shear but that they are coupled to each other.

While it is difficult to see from Fig. 6.20 the relative coupling of flexures to the $X_{y'}$ shear, experiment has shown the flexure modes along X to have the greater coupling to the $X_{y'}$ shear. This is true when the ratio $\frac{X}{Y'}$ is such that the flexure modes along X and high order Z'_x shear modes along X have their maximum separation. When these modes approach each other

and the $X_{y'}$ shear such as is shown in Fig. 6.21 at $\frac{X}{Y'} = 31.35$ the relative coupling of each to the $X_{y'}$ shear is about equal. This arises from the fact that the mutual coupling between them increases the apparent coupling

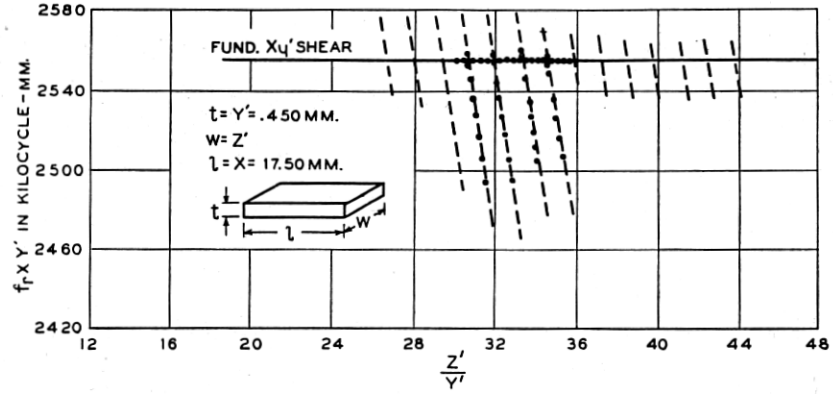

Fig. 6.19—High frequency shear resonances in a *BT*-cut plate.

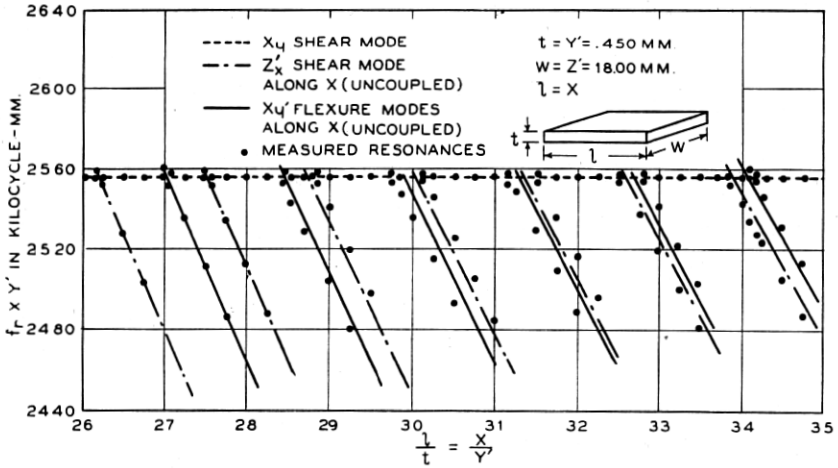

Fig. 6.20—High frequency thickness shear and flexure and shear resonances along the X axis in a *BT*-cut quartz plate.

between the $X_{y'}$ shear and high orders of Z'_x shear along X. From this it would appear advisable to avoid such regions in the dimensioning of crystals for oscillator use over wide temperature ranges. Determination of the flexure as well as high order Z'_x shears then must be made in regions where

they are spaced so that the effect of coupling between them will not influence the frequency constant that is determined experimentally. These regions have been investigated and the result for the flexure modes is that shown

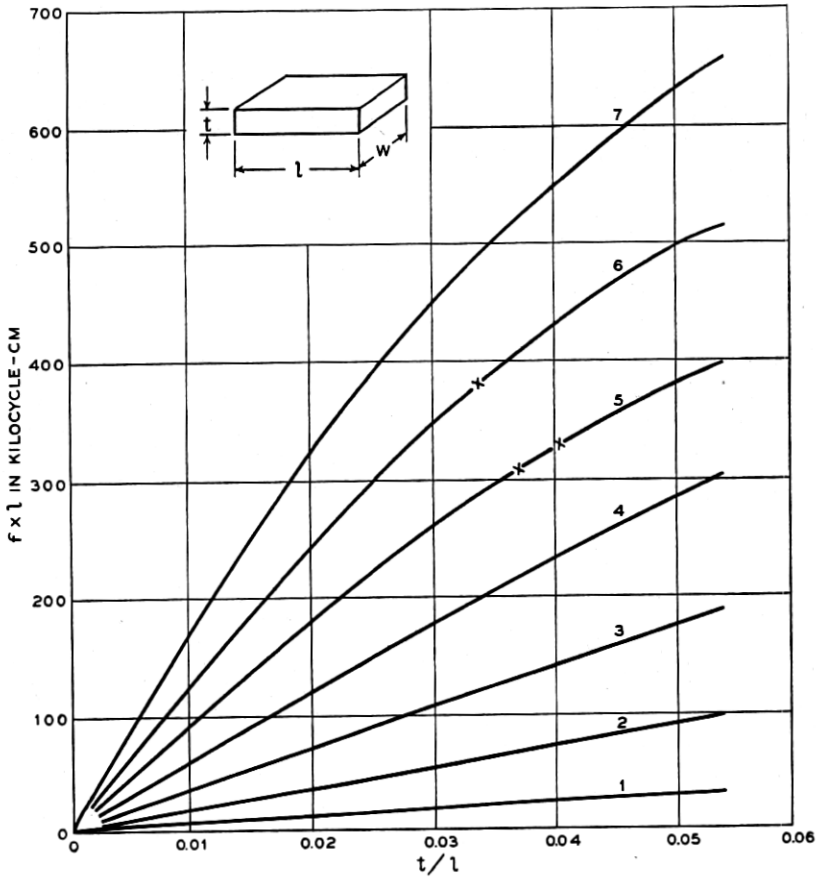

Fig. 6.21—Flexure resonances in a *GT*-cut quartz plate.

in equation 6.20. From Fig. 6.19 the high order Z'_x shears along Z' will be coincident with the high frequency $X_{y'}$ shear at frequencies given by

$$f_{z's} = \frac{166.45}{Z'} n_{z's} \quad \text{kilocycles} \qquad 6.27$$

From Fig. 6.20 high orders of the same Z'_x shear along X will be coincident with the high frequency X'_y shear at frequencies given by

$$f_{xs} = \frac{163.514}{X} n_{xs} \text{ kilocycles} \qquad 6.28$$

Upon substitution of the value of c'_{55} for a BT-cut in equation 6.22 there results

$$f_{t_s} \times \ell = \frac{1}{2}\sqrt{\frac{c'_{55}}{\rho}} = \frac{1}{2}\sqrt{\frac{30.3 \times 10^{10}}{2.65}} = 169.0 \text{ kilocycles} - \text{cm.}$$

which is 3.3% greater than that observed in equation 6.28 and 1.6% greater than that shown in equation 6.27. The apparent difference in the observed shear modulus in the X and Z' directions for the BT-cut can be explained from the fact that Young's modulus is quite different in the two directions for the BT-cut while it is nearly the same for the AT-cut as verified by equation 6.24 and 6.25.

From the discussion in this section it can be seen that a single theory that would relate all the now known resonances in quartz plates together with the effects of coupling would be prodigous indeed. In order to reduce the design of quartz plates to a simple engineering basis it is necessary to take specific examples and investigate the region in the vicinity of the frequency to be used based on general theory and then apply approximations that fit the specific cases.

6.5 Methods for Obtaining Isolated Modes of Motion

6.51 *GT Type Crystals*

In the case of GT type crystals the modes that cause the greatest concern are flexure modes in the two planes of the length and thickness and the width and thickness. The desired mode is that of an extensional mode along the width. To produce a low temperature coefficient it is also necessary that this mode be coupled to an extensional mode along the length, a fixed frequency difference from it. Therefore it will be necessary to prevent flexure modes from occurring at either of these two frequencies. Fig. 6.21 shows the frequency of various flexure modes that would be observed in GT-cut plates for different ratios of thickness to length. In the case of the GT-cut the elastic constants in the length and width directions are the same and therefore it is only necessary to determine the flexures in one plane to get a determination in both. From the plot of frequencies shown in Fig. 6.21, it would be very easy to determine the proper thickness for any given GT plate. Since in all practical cases there is a definite relation between the length and width of this type of plate, it would be necessary to examine the flexures in these two directions as a function of the change in thickness.

Fig. 6.22 shows a plot of this for the case of a *GT* crystal designed to operate at 164 kilocycles. All the information shown in this figure is obtained directly from Fig. 6.21. Since a change in thickness will not have any effect upon the length and width extensional modes of vibration and only

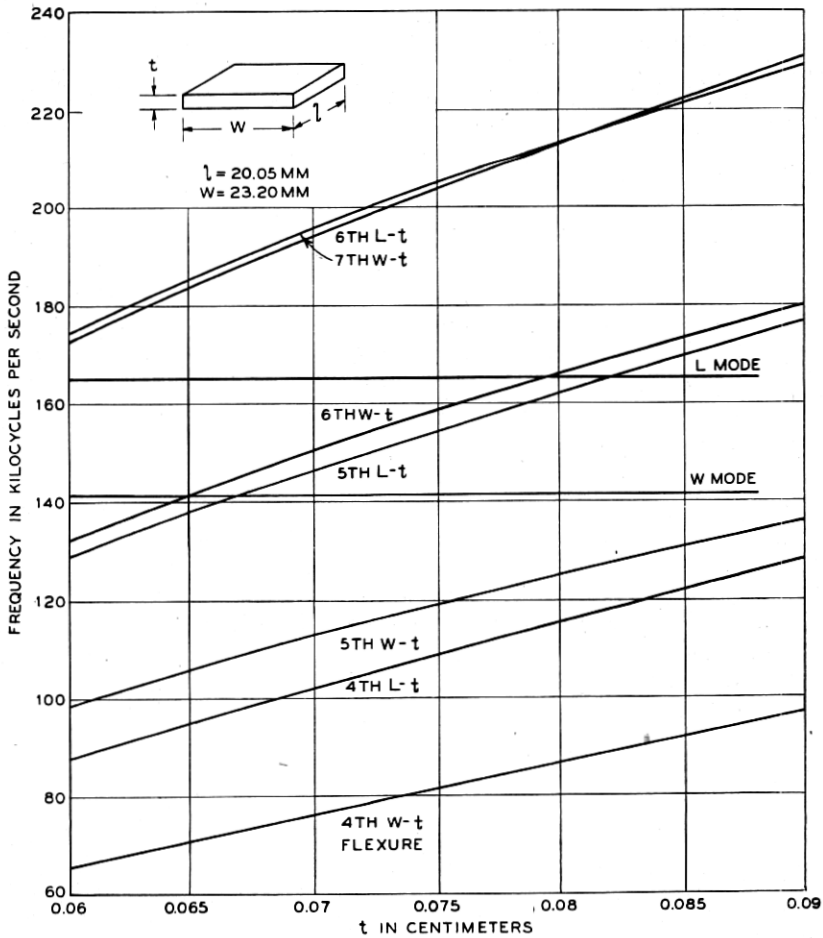

Fig. 6.22—Flexure and extensional resonances in a 164 kc *GT*-cut quartz plate.

changes the flexure frequencies, it would be reasonable to suppose that some thickness could be obtained where no flexure along the length or width would be of the same frequency as the length or width extensional mode. Examining the curves of Fig. 6.22, we find that a thickness of .06 cm., .075 cm. or .085 cm. would meet these conditions.

6.52 *BT Type Crystals*

As discussed in Section 6.4 the modes showing the greatest coupling to the high frequency thickness shear are of two types: high orders of $X_{y'}$ flexure propagated along the X axis and high order Z'_x shears along the X and Z' axes independently. Complex orders of the flexure and plate shear as illustrated in Fig. 6.2 and Fig. 6.4 do cause considerable difficulty and their analysis calls for special treatment and is not within the scope of this text. For the case of the BT-cut the three primary interfering series of modes are given by

$$f_{xf} = \frac{181.8}{X} n_{xf} \text{ kilocycles}$$

$$f_{xs} = \frac{163.514}{X} n_{xs} \text{ kilocycles} \qquad 6.30$$

$$f_{z's} = \frac{166.45}{Z'} n_{z's} \text{ kilocycles}$$

where X and Z' are given in centimeters and f_{xf} is the frequency at which integral orders of flexure modes along the X axis would coincide with the high frequency thickness shear mode. In a similar manner f_{xs} and $f_{z's}$ relate the same conditions for integral orders of the plate shear modes. These equations are true only in the case where the thickness is of such a value as to place the high frequency thickness shear mode at the same frequency as the computed interfering mode. In most practical cases for oscillator use the electric field is applied to the crystal by means of a flat electrode on each side of the crystal plate. Under this condition only odd order $X_{y'}$ shear modes along the X axis are excited and hence the strongest couplings to the $X_{y'}$ flexure modes will be only for even order values of n_{xf} in equation 6.30. In a similar manner the greatest interference between the $X_{y'}$ shear mode and high orders of the Z'_x shear modes along both X and Z' will occur for odd orders. Therefore the strongest interference from these modes will occur only for odd integers of n_{xs} and $n_{z's}$ in equation 6.30. These assumptions of only even flexures and odd shears showing appreciable coupling are based upon a crystal plate cut precisely along its proper axis and of uniform contour assembled in a holder using electrodes of uniform air gap. Deviations from these conditions will of course alter the ideal results dependent upon the amount and type of deviation.

The relationships shown in equation 6.30 may be more clearly seen when plotted graphically. Assuming a BT-cut crystal plate 1 centimeter square we may determine the frequencies at which an interfering mode will coincide with the high frequency $X_{y'}$ shear by assigning even integers to n_{xf} and odd

integers to n_{xs} and $n_{z's}$. Fig. 6.23 shows a plot of these three types of interfering modes on a folded frequency scale covering the range from 5 to 15 megacycles for a plate 1 centimeter square. Each abscissae covers a range of one megacycle with dots at three levels. The first level shows the frequencies at which successive even orders of flexure along the X axis occurs. The second level shows successive odd Z'_x shear modes along X and the third level successive odd Z'_x shear modes along Z'. The circles shown on the three levels indicate the results of actual measurements on BT-cut crystals as resonating elements. It will be noticed that the circles and dots coincide for most frequencies, the regions of departure occur only when a high order shear mode and a high order flexure mode along the X axis approach each

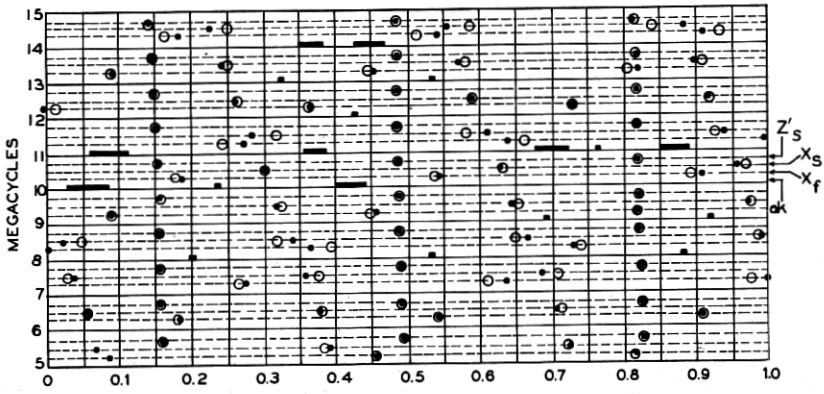

Fig. 6.23—Frequencies at which the Z'_x shear along X, the Z'_x shear along Z' and the X_y flexure along X coincide with the high frequency X_y shear in BT-cut crystals.

other in frequency. The reason for this is obvious from the previous discussion on the coupling between flexure and shear modes of motion.

The chart of Fig. 6.23 is of course not limited to a crystal 1 centimeter square or for that matter even a square crystal. In reality it relates the product of the frequency and X and Z' dimensions. For example a flexure mode interferes with the high frequency shear mode at a frequency of 9.45 megacycles for a plate with X dimension equal to 1 centimeter. If the X and Y' dimensions were doubled the same situation would exist at one half the frequency. In determining the dimensions for a crystal at a given frequency we know that the product of the frequency and X dimensions as well as Z' dimension must not result in a frequency close to those given by the circles of Fig. 6.23. In addition other interfering modes as previously mentioned must be avoided. These at present may be determined experimentally by choosing regions on the chart clear of the known flexure and shear modes.

On the abscissae are shown certain discreet frequencies as well as frequency ranges which have been found to result in crystal units having no serious dips in activity over a wide range in temperature. These are for square crystals in the 18 millimeter size range and have been obtained by Mr. G. M. Thurston of the Bell Laboratories and Mr. F. W. Schramm of the Western Electric Company. It will be noted that no so-called ok regions have been found at the frequencies of the three principal coupled modes.

While the use of the chart shown in Fig. 6.23 will often lead directly to the proper X and Z' dimensions for a given oscillator it cannot be overemphasized that only the three principal interfering modes are shown and only the odd orders for the shears and only the even orders for the flexure modes. Since the even order shear modes are excited due to slight variations which would produce wedge shaped air gaps or quartz blanks, it is advisable to avoid these regions also. Complex combinations of the three principal modes as shown in Figs. 6.2 and 6.4 are also driven. Therefore when it is necessary to produce a crystal unit possessing the highest activity for a given area of quartz plate over an extended temperature range it is necessary to scan the supposed desirable regions shown in Fig. 6.23 by complete measurements on finished units of a given size and varying frequency or of constant frequency and varying size. As an illustration the region shown in Fig. 6.23 between 10.025 and 10.080 megacycles was determined in this manner with the use of crystal plates approximately 18 millimeters square. The use of crystals with other than square dimensions could undoubtedly have increased the range of this region but their use is undesirable from a manufacturing standpoint. Assuming that the electrodes and crystal holder permit a variation in size of the quartz plate from 17.20 millimeters to 18.20 millimeters this approved region will immediately specify the dimensions of crystals to cover the frequency range from 5508 to 5727 kilocycles. This also assumes crystal blanks cut to precise orientations with controlled contours and electrodes of uniform flatness and constant airgap. While the theory would indicate that the frequency range given above could be expanded to considerably higher values by utilizing a smaller crystal blank this has not been proven so far since most crystals produced by the Western Electric Company require large area plates to meet high activity requirements.

As an illustration of the effect on the behavior of oscillators of changing the X and Z' dimensions of BT-cut quartz plates measurements have been made of the activity, in a conventional tuned plate circuit with the crystal connected between grid and cathode of quartz plates of constant thickness and varying X and Z' dimensions. Fig. 6.24 shows the effect of changing the X dimension of a quartz plate on its activity as an oscillator. By taking the product of the frequency and dimension we can determine the dimen-

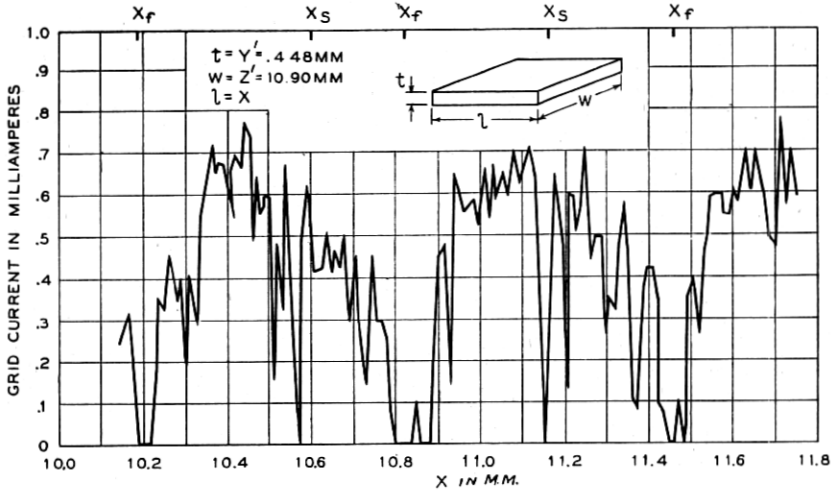

Fig. 6.24—Effect of change in X dimension on the activity of a BT-cut quartz plate in an oscillating circuit.

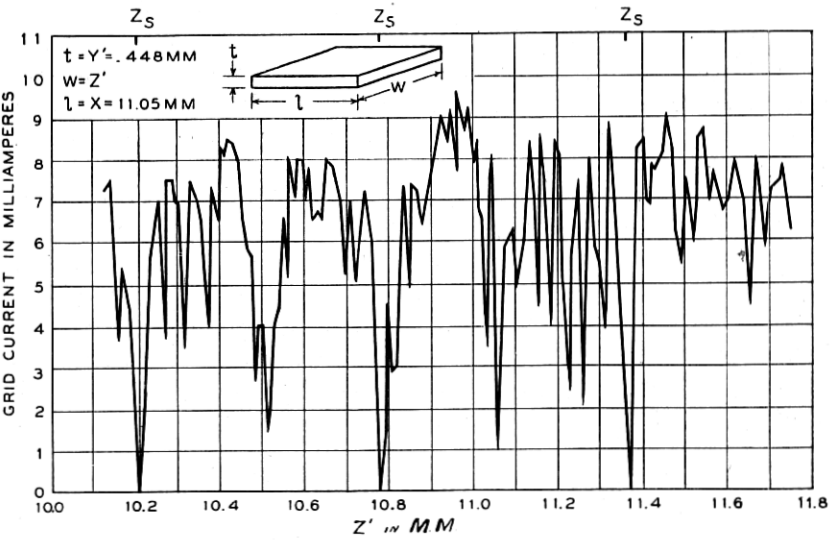

Fig. 6.25—Effect of change in Z' dimension on the activity of a BT-cut quartz plate in an oscillating circuit.

sions from Fig. 6.27 for this case where the $X_{y'}$ flexures and Z'_x shears will interfere to produce poor characteristics. These are shown in Fig. 6.24 for flexure modes as X_f and for the shear modes as X_s and do in general cor-

respond to the dimensions resulting in low or no activity. This illustrates quite clearly the necessity for grinding the edges of plates not dimensioned for a specific frequency. Fig. 6.25 shows the same conditions when only the Z' dimension is changed. In this case the dimensions shown at regular intervals as Z_s were derived from Fig. 6.25 as before and correspond to the zero activity dimensions found experimentally. It will be noticed that low activity regions are found halfway between the dimensions designated as Z_s. These correspond to even orders of the Z'_x shear and are the result of a slight wedge in the airgap. This was intentional to show the existence of this condition.

Figures 6.24 and 6.25 show the necessity for avoiding certain dimensions for oscillator plates at specific frequencies. This can be accomplished by

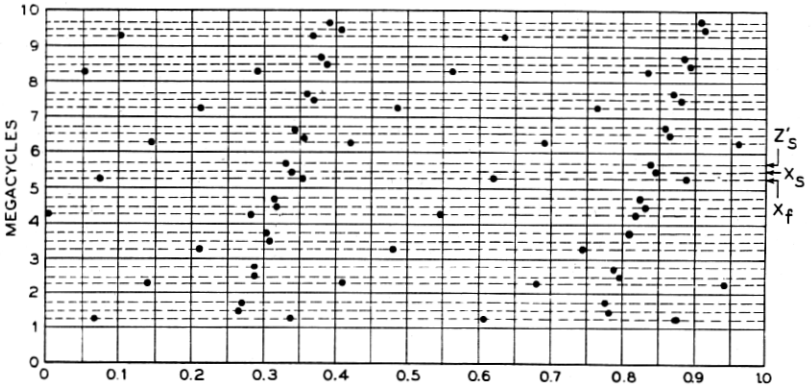

Fig. 6.26—Frequencies at which the Z'_x shear along X, the Z'_x shear along Z' and the X_y flexure along X coincide with the high frequency X_y shear in AT-cut plates.

individually adjusting the X and Z' dimensions by hand grinding of each plate or by predetermining the proper dimensions and using mass production methods of precise machine grinding. The advantages of predimensioned crystal units is the insurance of proper operation over a wide temperature range and uniformity of activity. The experience of most manufacturers of low frequency crystal units in the broadcast range and high frequency crystals requiring high activity over a wide temperature range has been that it is necessary to use specific dimensions to insure low rejects in the final tests.

6.53 *AT-Type Crystals*

The modes of motion encountered in the AT-cut crystal are the same as that of the BT-cut. The effects of coupling between most modes is greater

due to the increased piezo electric constant for this particular cut, and the frequency constants are different due to the change in angle with respect to the crystallographic axes. The three series of interfering modes as described for the BT-cut have been measured for this crystal and as shown in Section 6.4 are

$$f_{xf} = \frac{133.84}{X} n_{xf}$$

$$f_{xs} = \frac{254.20}{X} n_{xs} \qquad 6.31$$

$$f_{x's} = \frac{254.00}{Z'} n_{x's}$$

In a manner similar to the BT case a chart has been developed of a folded frequency scale showing the frequencies at which even order $X_{y'}$ flexure modes propagated along X and odd order Z'_x shear modes along X as well as odd order Z'_x shear modes along Z' will interfere with the high frequency $X_{y'}$ shear mode for a crystal 1 centimeter square. This is shown in Fig. 6.26. Its use is the same as that described for the BT case. Insufficient experimental work has been done to indicate the relative shift in the flexure and shear modes along the X axis when they approach each other in frequency. Also, most of the use of square plates and experimental work has been confined to the BT-cut crystals and hence no ok regions are shown for this chart.

APPENDIX B

Equation of elastic and piezoelectric constants for rotation of axes about the X axis. ($s = \sin\theta$; $c = \cos\theta$)

$$c'_{11} = c_{11}$$

$$c'_{22} = c_{11}c^4 + c_{33}s^4 + 2(2c_{44} + c_{13})s^2c^2 + 4c_{14}sc^3$$

$$c'_{33} = c_{11}s^4 + c_{33}c^4 + 2(2c_{44} + c_{13})s^2c^2 - 4c_{14}s^3c$$

$$c'_{44} = c_{44} + (c_{11} + c_{33} - 4c_{44} - 2c_{13})s^2c^2 - 2c_{14}(c^2 - s^2)\,sc$$

$$c'_{55} = c_{44}c^2 + c_{66}s^2 + 2c_{14}sc$$

$$c'_{66} = c_{44}s^2 + c_{66}c^2 - 2c_{14}sc$$

$$c'_{12} = c_{12}c^2 + c_{13}s^2 - 2c_{14}sc$$

$$c'_{13} = c_{12}s^2 + c_{13}c^2 + 2c_{14}sc$$

$$c'_{14} = c_{14}(c^2 - s^2) + (c_{12} - c_{13})sc$$

$$c'_{23} = c_{13}(c^4 + s^4) + (c_{11} + c_{33} - 4c_{44})s^2c^2 - 2c_{14}(c^2 - s^2)sc$$

$$c'_{24} = c_{14}(4s^2 - 1)c^2 + [c_{11}c^2 - c_{33}s^2 - (2c_{44} + c_{13})(c^2 - s^2)]sc$$

$$c'_{34} = -c_{14}(4c^2 - 1)s^2 + [c_{11}s^2 - c_{33}c^2 + (2c_{44} + c_{13})(c^2 - s^2)]sc$$

$$c'_{56} = c_{14}(c^2 - s^2) + (c_{66} - c_{44})sc$$

$$c'_{15} = c'_{16} = c'_{25} = c'_{26} = c'_{35} = c'_{36} = c'_{45} = c'_{46} = 0$$

$$s'_{11} = s_{11}$$

$$s'_{22} = s_{11}c^4 + s_{33}s^4 + (s_{44} + 2s_{13})s^2c^2 + 2s_{14}sc^3$$

$$s'_{33} = s_{11}s^4 + s_{33}c^4 + (s_{44} + 2s_{13})s^2c^2 - 2s_{14}s^3c$$

$$s'_{44} = s_{44} + 4(s_{11} + s_{33} - s_{44} - 2s_{13})s^2c^2 - 4s_{14}(c^2 - s^2)sc$$

$$s'_{55} = s_{44}c^2 + s_{66}s^2 + 4s_{14}sc$$

$$s'_{66} = s_{44}s^2 + s_{66}c^2 - 4s_{14}sc$$

$$s'_{12} = s_{12}c^2 + s_{13}s^2 - s_{14}sc$$

$$s'_{13} = s_{12}s^2 + s_{13}c^2 + s_{14}sc$$

$$s'_{14} = s_{14}(c^2 - s^2) + 2(s_{12} - s_{13})sc$$

$$s'_{23} = s_{13}(c^4 + s^4) + (s_{11} + s_{33} - s_{44})s^2c^2 - s_{14}(c^2 - s^2)sc$$

$$s'_{24} = s_{14}(4s^2 - 1)c^2 + [2(s_{11}c^2 - s_{33}s^2) - (s_{44} + 2s_{13})(c^2 - s^2)]sc$$

$$s'_{34} = -s_{14}(4c^2 - 1)s^2 + [2(s_{11}s^2 - s_{33}c^2) + (s_{44} + 2s_{13})(c^2 - s^2)]sc$$

$$s'_{56} = 2s_{14}(c^2 - s^2) + (s_{66} - s_{44})sc$$

$$s'_{15} = s'_{16} = s'_{25} = s'_{26} = s'_{35} = s'_{36} = s'_{45} = s'_{46} = 0$$

$$d'_{11} = d_{11}$$

$$d'_{12} = -(d_{14}s + d_{11}c)c$$

$$d'_{13} = (d_{14}c - d_{11}s)s$$

$$d'_{14} = d_{14}(c^2 - s^2) - 2d_{11}sc$$

$$d'_{25} = -(d_{14}c + 2d_{11}s)c$$

$$d'_{26} = (d_{14}s - 2d_{11}c)c$$

$$d'_{35} = -(d_{14}c + 2d_{11}s)s$$

$$d'_{36} = (d_{14}s - 2d_{11}c)s$$

$$d'_{15} = d'_{16} = d'_{21} = d'_{22} = d'_{23} = d'_{24} = d'_{31} = d'_{32} = d'_{33} = d'_{34} = 0$$

$$e'_{11} = e_{11}$$

$$e'_{12} = -(2e_{14}s + e_{11}c)c$$

$$e'_{13} = (2e_{14}c - e_{11}s)s$$

$$e'_{14} = e_{14}(c^2 - s^2) - e_{11}sc$$

$$e'_{25} = -(e_{14}c + e_{11}s)c$$

$$e'_{26} = (e_{14}s - e_{11}c)c$$

$$e'_{35} = -(e_{14}c + e_{11}s)s$$

$$e'_{36} = (e_{14}s - e_{11}c)s$$

$$e'_{15} = e'_{16} = e'_{21} = e'_{22} = e'_{23} = e'_{24} = e'_{31} = e'_{32} = e'_{33} = e'_{34} = 0$$